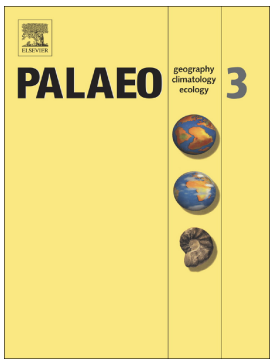

The relationship of plant leaf δ13Cn-alkanes and salinity in coastal ecosystems applied to palaeobotany: Case study from the Cenomanian of the Bohemian Cretaceous Basin, Czechia

Petra Zahajská, Jana Čepičková, Jakub Trubač, Nikolai Pedentchouk, Jiří Kvaček

PII: S0031-0182(24)00041-5

DOI: https://doi.org/10.1016/j.palaeo.2024.112052

Reference: PALAEO 112052

To appear in: *Palaeogeography, Palaeoclimatology, Palaeoecology*

Received date: 5 May 2023

Revised date: 16 January 2024

Accepted date: 18 January 2024

Please cite this article as: P. Zahajská, J. Čepičková, J. Trubač, et al., The relationship of plant leaf δ13Cn-alkanes and salinity in coastal ecosystems applied to palaeobotany: Case study from the Cenomanian of the Bohemian Cretaceous Basin, Czechia, *Palaeogeography, Palaeoclimatology, Palaeoecology* (2023), https://doi.org/10.1016/j.palaeo.2024.112052

The relationship of plant leaf $\delta^{13}C_n$–alkanes and salinity in coastal ecosystems applied to palaeobotany: Case study from the Cenomanian of the Bohemian Cretaceous Basin, Czechia

Petra Zahajská[a,b,*], Jana Čepičková[a], Jakub Trubač[c], Nikolai Pedentchouk[d], Jiří Kvaček[e]

[a]*Institute of Geology and Palaeontology, Faculty of Science, Charles University, Albertov 6, Prague, 128 43, Czechia*

[b]*Institute of Geography and Oeschger Center for Climate Change Research, University of Bern, Hallerstrasse 12, Bern, 3012, Switzerland*

[c]*Institute of Geochemistry, Mineralogy and Mineral Resources, Faculty of Science, Charles University, Albertov 6, Prague, 128 43, Czechia*

[d]*School of Environmental Sciences, University of East Anglia, Norwich, NR4 7TJ, United Kingdom*

[e]*National Museum, Václavské náměstí 68, Prague, 115 79, Czechia*

Abstract

Stable carbon isotopes in fossil leaf cuticles (*n*-alkanes, $\delta^{13}C_{n-alkanes}$) extracted from the sediment are widely used for palaeoenvironmental reconstructions. This approach relies on a series of assumptions (such as the plant-group-specific isotopic range, or the atmospheric CO_2 being the major factor for the isotopic values) and leaves out the complexity of the carbon isotope fractionation within the plant through time, space, and different environments. The leaf cuticle is a unique archive of local environmental conditions, which has the potential to constrain individual plant habitat. To explore the applicability of the information gained from the $\delta^{13}C_{n-alkanes}$ from fossil plants, a fossil coastal environment was studied.

During the Cenomanian (100.5-93.9 Ma), the basal part of the Bohemian Cretaceous Basin, including locality Pecínov (Czechia), was formed as a result of sea transgression to the Palaeozoic Bohemian Massif triggered by the Alpine orogenesis. Coastal halophytic vegetation growing in this zone of prograding sea has no extant equivalent, and there are uncertainties

* Corresponding author

Email address: petra.zahajska@unibe.ch (Petra Zahajská)

associated with vegetation distribution or individual taxa habitat.

Therefore, we examine the relationship between $\delta^{13}C_{n-alkanes}$ extracted from individual leaves of coastal C3 plants (fossil and modern) and osmotic stress (salinity and drought) to reconstruct the individual plant habitat, thus, vegetation distribution in the coastal zone. We investigated modern mangrove and salt marsh vegetation in New Zealand and the United Kingdom, respectively, as well as transition zones (mangrove invading original salt marshes) for $\delta^{13}C$, soil moisture and salinity to build a calibration of the relationship, which is then applied to the Cenomanian fossil leaves from the locality of Pecínov.

We found a positive correlation between water stress (caused by salinity or drought) and the $\delta^{13}C$ values of *n*-C_{25}, *n*-C_{27}, *n*-C_{29} and *n*-C_{31} alkanes when combining all species from all modern localities. However, the absence of a strong correlation within individual species suggests a combination of several factors controlling the carbon isotopic composition. Nevertheless, the general response of $\delta^{13}C$ to osmotic stress can be applied to compare the habitat of modern and fossil coastal plants. Thus, by using this relationship, we reconstructed the relative salinity and water stress of individual species of the Cenomanian plants by relating them to modern species-specific ranges of *n*-C_{29} isotopic signatures.

We showed that the $\delta^{13}C_{n-alkanes}$ of fossil plant cuticles/leaves can be a valuable tool in the reconstruction of plant habitat and help us understand evolution of fossil environments in time and space. Additionally, our data further confirm that the $\delta^{13}C$ acquired from plants should be used with caution when reconstructing global atmospheric CO_2 because the osmotic stress can shift the $\delta^{13}C$ in plants growing in terrestrial environments, particularly in coastal sea-influenced ecosystems.

Keywords: leaf waxes, carbon isotopes, salinity, osmotic stress, the Cenomanian, coastal environment

1. Introduction

Carbon isotopes from plant tissues are used for measurements of physiological, environmental and palaeoenvironmental variables such as atmospheric CO_2 concentration, light

availability, temperature, and water use efficiency (reviewed in Dawson et al., 2002; Arens et al., 2000; Wang et al., 2018; Rao et al., 2017; Cernusak et al., 2013; Yan et al., 2020). With the technological advances, the stable carbon isotopes are now commonly measured on a compound level, e.g. *n*-alkanes, which provide us with more specific information about the plant metabolism, and are used for paleoclimate and paleoecology reconstructions (e.g., McInerney et al., 2011; Badewien et al., 2015; Wang et al., 2022; Kohn, 2010, and many more). Algae and bacteria mainly produce short-chain alkanes (n-C_{19}, n-C_{21}, Cranwell et al., 1987), mid-chain alkanes (n-C_{23}, n-C_{25}) are typical for aquatic plants (Ficken et al., 2000), and long-chain alkanes (n-C_{29} - n-C_{33}) are abundant in terrestrial higher plants (Eglinton and Hamilton, 1967). The use of long-chain alkanes for palaeoreconstructions increased rapidly since the first results showed their high preservation potential (Eglinton et al., 1991; Peters et al., 2005; Bush and McInerney, 2013) and that the signal of the water use efficiency is also preserved in bulk plant material (Bocherens et al., 1993; Tu et al., 2004).

Traditional estimates of palaeoecology of fossil plants are usually based on leaf morphology (shape, size, rim, venation), micromorphology of fossil plant cuticle (Watson and Alvin, 1996; Čepičková and Kvaček, 2020), or growth rings (Greguš et al., 2020). Indirect signals are based also on combination of palaeobotanical observations and studies on palynology and sedimentology (Uličný et al., 1997b). More direct palaeoecological signal comes with analytical methods, such as stable carbon isotopes. Nowadays, many studies work on bulk or compound specific organic matter signal, which serves well for the regional palaeoreconstructions as it integrates the effect of all environmental factors (Liu et al., 2022; Castañeda and Schouten, 2011). However, to reconstruct individual plant habitat, which is often crucial in palaeobotanical species interpretation and thus vegetation distribution reconstruction, we need to implement more specific toolbox.

The use of individual plant leaves to analyse the $\delta^{13}C$ in *n*-alkanes, allows to compare recent and fossil data on the same compound, not only the leaf bulk. We target the n-C_{29} as it is most common homologue used in palaeoenvironmental studies (e.g., Sachse et al., 2012), as well as most commonly abundant *n*-alkane for targeted taxa – gymnosperms and angiosperms, woody and non-woody plants (Liu et al., 2022; Diefendorf and Freimuth, 2017). Additionally, the $\delta^{13}C$ in n-C_{29} was shown to have stronger relationship with the water use efficiency than with the bulk

plant material (Liu et al., 2019) and the $\delta^{13}C$ in $n\text{-}C_{n-alkanes}$ showed response on salinity gradient (Ladd and Sachs, 2013; He et al., 2021). Specially for fossil record, where organic matter undergoes decomposition and faces diagenetic processes, it is important to target only one specific and stable compound to decrease the bias from other potentially preserved compounds (Eley et al., 2018). Based on that knowledge, we aim to continue in the effort to develop a new palaeoproxy constraining the gradient of relative water use efficiency for individual fossil plants by calibrating the $\delta^{13}C$ of long-chain *n*-alkanes on modern and fossil coastal plant material. Whilst using fossil plant material we target only C3 modern plant species for the calibration dataset, as the first C4 plants appeared generally after the mid-Cretaceous (Sage, 2004).

The most suitable natural gradient for water use efficiency is the coastal salt marsh or mangrove ecosystem demonstrated in the leaf wax isotopic composition reacting on osmotic stress in saltmarshes (Eley et al., 2016), mangrove cultivations (Park et al., 2019) and in the natural mangroves (Ladd and Sachs, 2013; He et al., 2022). As a fossil representative, we have investigated the Cenomanian (100.5-93.9 Ma) deltaic system of the Cretaceous Basin in locality Pecínov, Czechia. This locality is sedimentologically (Uličný et al., 1997b) and palaeobotanically (Kvaček, 1999a, 2000; Kvaček et al., 2005, 2016; Tu et al., 2004; Coiffard et al., 2006) well-studied and described as a deltaic environment with temporal prograding sea, which affects the vegetation composition and distribution (Uličný and Špičáková, 1996; Uličný et al., 1996; 63 Uličný et al., 1997b).

We sampled plants growing in modern environments which are the closest analogues to the fossil environments (based on Uličný et al., 1997b) for salinity and stable carbon isotopes in the plant leaves to investigate their relationship. We hypothesize that with an increasing salinity, most species will show isotopically heavier/higher values due to osmotic stress – enclosure of stomata and thus, the increased water use efficiency. This was previously showed in mangrove ecosystems (Farquhar et al., 1982; Ladd and Sachs, 2013; Park et al., 2019; He et al., 2022) as well as in salt marshes (Eley et al., 2016). We expand and build on these studies to constrain more of the coastal ecosystem types and to build a modern calibration data. Further, we use this modern calibration dataset combined with published cuticular data to reconstruct the Cenomanian coastal plant habitat, mainly to identify the osmotic stress (water availability and salinity) for each sample and species as well as for plant community of each sedimentological unit.

2. Study sites & Methods

2.1. Fossil locality and choosing its analogue

Fossil plants samples originate from the Late Cretaceous, the Cenomanian deposits of the Peruc-Korycany Formaion within the Bohemian Cretaceous Basin as defined by Čech (2011) from Pecínov quarry (50°07’55"N 13°54’36"E) situated 50 km west of Prague (Uličný et al., 1997b, et al., 2006). During the Cenomanian (100.5-93.9 Ma), the Bohemian Cretaceous Basin was formed as a result of sea transgression to the Palaeozoic Bohemian Massif triggered by the Alpine orogenesis (Uličný et al., 2009). The most basal sediments of the basin are assigned to the Peruc–Korycany Formation. They represent a transgretional set of sedimentary bodies which record gradual inundation of the massif by sea from east and north. The most basal position is occupied by terrestrial fluvial sediments containing both the alluvial plain and upland vegetation. They are assigned to Unit 1 (Uličný et al., 1997b). Fluvial sediments of Unit 2 show partial sea influence (tidally influenced river) and generally alluvial plain vegetation. Deposits of coastal swamp (U3a), salt marsh (U3b) and tidal channels (U3c) are characterised by mudstones rich in organic material. Their plant content recorded ranges from swamp vegetation to halophytic vegetation. Sediments of Unit 4 were formed in tidal flats and salt marshes in coastal swamp, sediments of Unit 5 by coastal swamp. (Uličný et al., 1997b).

Palaeoclimate of the Peruc Flora that is found in the Pecínov quarry is interpreted as paratropical, seasonally dry (Falcon-Lang et al., 2001; Greguš et al., 2020) with mean annual temperatures about 17-20°C (Kvaček et al., 2002; Herman et al., 2002). The proxy-parameters for the Peruc Flora produced by CLAMP are as follows: Mean annual temperature: 17°C, warm month mean temperature: 23°C, cold month mean temperature: 11°C, mean annual precipitation: 1468 mm, precipitation during driest three months: 180 mm, growing season length: 9.5 months. These climate parameters are comparable with those calculated by computer models – warm month mean temperature 20-24°C and cold month mean temperature 12-16°C (Valdes et al., 1996).

Our collection of samples was chosen to cover five sedimentary units that represent the whole evolution of coast from fluvial and tide-influenced fluvial sediments in Unit 1 and 2, respectively, through salt marsh-like environment in Unit 3, to coastal swamp in Unit 5 (Table 1 Uličný et al., 1997b).

Table 1: Table of palaeoenvironments derived from (Uličný et al., 1997b) and species sampled from these units.

Unit	Palaeoenvironmet	Sampled species
U1	Braided river, allochthonous material from slopes and upland	*Ceratoxylon*, *Eucalyptolaurus*, *Nilssonia mirovanae*, *Pandemophyllum*, *Papillaephyllum labutae*, *Pseudoctenis babinensis*
U2	Tidally influenced braided river	*Araliaeophyllum*, *Ettingshausenia laevis*, *Eucalyptolaurus*, *Pandemophyllum*
U3a	Coastal swamp	Not sampled, represented by species in U5
U3b	Supratidal salt marsh	*Diospyros cretacea*, *Eretmophyllum obtusum*, *Frenelopsis alata*, *Pseudoasterophyllites cretaceus*
U3c	Channel infills, allochthonous material from slopes and upland	*Ascarinophyllum pecinovense*, *Eucalyptolaurus*, *Pandemophyllum*
U4	Tidal flat	Not sampled
U5	Coastal swamp	*Cunninghamites lignitum*, *Sphenolepis pecinovensis*

Leaves of selected fossil plants (Table 1 and A.4) were collected directly in the field and further subsampled by separating the plant material mechanically from the embedding mudstone (Uličný et al., 1997b). Some samples rich in fossil material were bulk macerated using water with sodium carbonate (Na_2CO_3). Subsamples were cleaned in MQ water and HF (40%) for 5 to 10 minutes to remove any potential sediment contamination. Samples were then analysed for their cuticles (no in this study, Čepičková and Kvaček, 2023, in review; Čepičková and Kvaček, 2022)

which are here used as an independent proxy for the plant habitat determination complementary to the data from extracted *n*-alkanes (see Method section 2.3 below).

To constrain the salinity stress in these fossil environments, analogous environments with modern plant species were investigated. However, there is no modern analogous (in terms of basin morphology combined with climate and taxonomy) environmental setting to Unit 3, as the salt marsh-like Unit 3b was inhabited by small coniferous species, angiosperm trees and ginkgoes (Uličný et al., 1997b; Kvaček, 2000; Kvaček et al., 2005, 2012, 2016). The only close analogous environments to the Cretaceous succession are modern alluvial plains, riverbanks, salt marshes, mangroves, and mostly salt marshes invaded by mangrove trees. Therefore, modern deltas, coastal dunes, salt marshes of the United Kingdom, with addition of mangroves, and salt marshes invaded by mangrove trees of New Zealand were chosen and sampled as the closest analogues to the fossil sedimentary environments observed in Pecínov.

2.2. Modern study sites

During period of one week in summer 2015, salt marshes of the United Kingdom (Figure 1A) were sampled for whole leaves of 6 species (Table 2). The mean annual temperature (MAT) of these three localites are ranging from 9 to 11°C and precipitation (MAP) between 730 to 1300mm (source metoffice.gov.uk, accessed 04/01/2024). Further, during period of two weeks in December 2017, whole leaves of 11 species (Table 2) together with a sample of substrate/soil in which the plants were growing and data on pH measured on-site, were collected on New Zealand's coastal ecosystems (Figure 1B). The MAT of these 12 localities is ranging from 13 to 16°C and MAP between 800 to 1500mm (source niwa.co.nz, accessed 04/01/2024). *Plantago lanceolata* was collected at all localities, when found, as a control species.

Figure 1: Map of all modern study sites, which were sampled as the closest analogue of the Cenomanian coastal environment. Five different types of coastal environments were sampled: Blue square represents coastal deltas, orange small circle shows mangroves, green triangles are the salt marshes, yellow diamond is used for coastal dunes and purple big circle represents the salt marshes invaded by mangrove trees called here transition zone. Inset (A): Map of the United Kingdom with three sampled salt marshes: King's Lynn, Grange-over-Sands and Little Neston. Inset (B): Five types of coastal environment found on New Zealand's northern island as potential

analogues and calibration set for the Cenomanian locality. Five mangroves in the northern part of the northern island, four salt marshes in the middle and southern part of the island, three transition zones situated in the middle part of the island, one delta, and one coastal dunes environment further south on the island were sampled for plants and soils.

The soil samples were analysed for their water content gravimetrically after air-drying. Air-dried samples were used for measuring salinity in 1:5 soil:water extract (Hardie and Doyle, 2012). In brief, eight grams of air-dried soil was suspended in 40 ml of deionized water, mechanically shaken for 30 minutes and after 15 minutes of settling, the supernatant conductivity and temperature were measured. The electrical conductivity data ($EC_{1:5}$) were converted to EC saturated paste extract (EC_{eq}) and corrected for temperature differences (Rayment et al., 1992; Hardie and Doyle, 2012).

Table 2: List of all sampled species, the sampling locality, characteristic environment and salinity of the soils. *Invaded salt marsh by mangrove trees.

Species	Locality	Environment	Salinity $EC_{eq}(dS \cdot m^{-1})$
Plantago coronopus	New Zealand	Delta, Salt marsh, Transition*, Coastal dunes	Min. 0.4, Max. 31, Average 4.8
Avicennia marina/rensifera	New Zealand	Mangrove	Min. 18, Max. 208, Average 58
Armeria martima	Great Britain	Salt marsh	Not measured
Calystegia soldanella	New Zealand	Salt marsh	0.2
Coprosma repens	New Zealand	Salt marsh	Min. 3.4, Max. 23, Average 10
Glaux maritima = *Lysimachia maritima*	Great Britain	Salt marsh	Not measured

Halimione portulacoides = *Atriplex portulacoides*	Great Britain	Salt marsh	Not measured
Pittosporum crassifolium	New Zealand	Salt marsh	4.2
Plantago maritima	Great Britain	Salt marsh	Not measured
Salicornia maritima	Great Britain	Salt marsh	Not measured
Triglochin striata	New Zealand	Salt marsh, Coastal dunes, Mangrove	Min. 7.6, Max. 83, Average 59
Glossostigma elatinoides	New Zealand	Salt marsh, Mangrove, Transition*	Min. 20, Max. 61, Average 38
Sueda maritima	Great Britain and New Zealand	Salt marsh, Transition*	36
Samolus repens	New Zealand	Salt marsh, Transition*, Coastal dunes, Mangrove	Min. 7.5, Max. 138, Average 42
Salicornia australis = *Salicornia quinqueflora*	New Zealand	Salt marsh, Transition*, Mangrove	Min. 2, Max. 138, Average 44
Plantago lanceolata	New Zealand	Salt marsh, Transition*, Out of marsh = control	Min. 0.6, Max. 41, Average 15

2.3. Extraction of n-alkanes from plant material

The extraction of *n*-alkanes from the plant material was done according to the method of Eley et al. (2014). Briefly, the total lipid fraction was obtained from the leaf material (between 1 cm^2, up to whole plant) by sonication for 30 minutes, in case of recent material, and two times 30-45 minutes in case of fossil material in HPLC or GC grade hexane. The amount of material depends on size of leaves, ranging between a fossil leaf fragment of 1 cm^2, 5 recent leaves and

whole plant (e.g., *Salicornia australis*). However, for fossil material, there is only a limited amount of material available. Further, the amount of material used depends on the thickness of the cuticle, which is only a part of the entire plant leaf. Therefore, we were not able to quantify exact amount of the cuticle material used for extraction per sample. Leaves were separated from the solution, which was further concentrated to 1 ml under high-grade nitrogen gas (Nitrogen purity 4, Linde) in heated (40°C) thermoblock. Full chemical replicates of each sample were extracted to ensure the reproducibility. If, for lack of material, full chemical replicates could not be extracted, analytical replicates from the same leaf material were extracted, by repetitive sonication.

The *n*-alkane fraction was eluted with HPLC/GC grade hexane during column chromatography. A glass Pasteur pipette (150 mm long) was packed with silica gel (high-purity grade (Davisil Grade 635); pore size 60 Å; 60-100 mesh, 150-250 μm; Sigma-Aldrich) and the total lipid extract (1 ml) was loaded onto the activated column. The column was activated and eluted, before and after, respectively, with 5-6 ml of hexane and the final eluent containing *n*-alkanes was collected in 8 ml-glass vials (Labicom). For column chromatography an SPE Manifold (Waters) with 12 positions was used. Eluents were concentrated under the stream of high-grade nitrogen (Nitrogen purity 4, Linde) whilst heated in the thermoblock to 40°C. Samples were completely evaporated and then dissolved in 100 μl of hexane. The fossil samples were washed by 300 μl and blown down again under the nitrogen in the thermoblock for the final volume of 100 μl. The final volume was injected into 350 μl inserts (Labicom) placed in 1.8 ml HPLC vials (Labicom). Samples were stored in a fridge until GC-MS and GC-IRMS analyses.

2.4. Stable carbon isotopes analyses of plant material

The extracted and purified *n*-alkanes were measured for their stable carbon isotopes using a Delta V Advantage ThermoFisher Scientific isotope-ratio mass spectrometer interfaced by GC-Isolink II Trace with GC combustion and high temperature conversion systems, using the capillary column (Restek DB-5MS, length 30 m, ID 0.25 mm, df 0.25 μm) at the Stable and Radiogenic Isotope Laboratory at Charles University, Prague. The oven temperature was raised from 50°C to 210°C at 15°C min^{-1}, then at 7°C min^{-1} to 320°C. *n*-alkanes were identified by comparison of their elution times with *n*-C_{16} to *n*-C_{30} standard mix A6 (A. Schimmelmann, Biogeochemical Laboratories, Indiana University). $\delta^{13}C$ values of *n*-alkanes are reported based

on replicate analysis of well-resolved peaks and expressed relative to Vienna Pee Dee Belemnite (VPDB) based in in-house reference gasses CO_2 adjusted daily using a standard mixture of *n*-C_{16} to *n*-C_{30} alkanes. Reproducibility of reference gas peak CO_2 $\delta^{13}C$ values (analysed at the beginning and end of each sample measurement) did not exceed ± 0.063. Differences between repeat measurements of the same analytical sample did not exceed 10. Root mean square errors for standard measurements (*n*-C_{16} to *n*-C_{30} alkanes) did not exceed 0.40 (n = 120) throughout sample analysis. To assess the heterogeneity of the carbon isotope composition of a single plant species, we analysed two of the sample replicates we collected for each plant, and calculated the absolute difference in $\delta^{13}C$ values between these measurements. For all species, this variability did not exceed 10%. The total number of measured samples including replicates was 364.

2.5. Data processing and statistical analyses

The data from the GC-IRMS analysis were processed in ThermoScientific Workspace software, MS Excel and plotted in R. The *n*-alkanes were identified based on retention times of peaks in measured *n*-C_{16} to *n*-C_{30} alkanes standard mix A6 (A. Schimmelmann, Biogeochemical Laboratories, Indiana University). The most common alkanes were *n*-C_{25}, *n*-C_{27}, *n*-C_{29} and *n*-C_{31}. Some of the samples had also high peak in retention time of *n*-C_{31} or *n*-C_{33}, but these alkanes could not be used for comparing with the fossil samples. After the detection of *n*-alkanes, the sample replicates were used for determining the sample natural variability and reproducibility, which is within 10%.

Pearson's ans Spearman's correlation test was run on the whole dataset, separate species and chosen *n*-alkanes in species to identify correlations. The statistical significance all correlations were tested in R software. A statistically significant correlation was considered to have a confidence interval of 95% and thus, the p-value < 0.05. We tested the data for normality using Q-Q test and further conducted a series of statistical tests (t-test, variance F-test, Kolmogorov-Smirnov test, and ANOVA) to evaluate the significance of the variation of $\delta^{13}C$ and salinity between individual species and locality types. Additionally, we build linear and generalized linear model to test the relationship between the $\delta^{13}C$ and salinity. As the salinity data are not normally distributed, we used the linear mixing models and Monte Carlo linear model

to evaluate the significance of the relationship between $\delta^{13}C$ and salinity.

The recent data were tested for phylogenetic autocorrelation using Abouheif's test (Abouheif, 1999; Pavoine et al., 2008) in R package adephylo (Jombart et al., 2010). We have conducted ordinary least squares regression on the whole dataset and phylogenetic generalized squares on the mean and median of the isotopic data and salinities assigned to the phylogenetic tree tips.

2.6. Correction for $\delta^{13}C_{air}$ values

To be able to better compare the absolute differences of isotopic signals between fossil and modern plant species and environments, we have applied the correction of variable $\delta^{13}C_{air}$ value through time (Barral et al., 2017) on the plant material $\delta^{13}C_{plant}$ resulting in a fractionation factor $\Delta^{13}C$ as follows (Farquhar et al., 1989):

$$\Delta^{13}C = \frac{\delta^{13}C_{air} - \delta^{13}C_{plant}}{1 + \delta^{13}C_{plant}}, \quad (1)$$

where $\delta^{13}C_{air}$ used for the Cretaceous is -4.970 (Barral et al., 2017) and current $\delta^{13}C_{air}$ is -8.45 (He et al., 2021). We used our $\delta^{13}C_{n\text{-}C_{29}}$ as the $\delta^{13}C_{plant}$ values.

3. Results

3.1. The relationship between salinity and cuticular n-alkane $\delta^{13}C$ of modern coastal species

Data of $\delta^{13}C$ in n-C_{29} from all recent samples (n = 281) show variation within a range from -27.40 to -40.10 with an average of -33.20 and median of -32.90 (Figure 3.1 and 2). This is slightly higher number compared to our control, non-osmotically stressed, species *Plantago lanceolata* ranging from -31.5 to -38.40 with an average value -36.60. Thus, we can consider this value as a reference of non-stressed C3 plant.

Out of 11 species, two show positive correlation between salinity and all *n*-alkanes (n-C_{16} - n-C_{31}): *Salicornia australis* and *Avicennia rensifora* show weak, but significant positive correlation (R^2_{Sal} =0.036 and R^2_{Avi} =0.115, respectively) when all localities are used. *Salicornia*

australis additionally shows positive correlation for n-C_{25}, n-C_{27}, n-C_{29} and n-C_{31} ($R^2_{n\text{-}C_{25}}$ =0.24, $R^2_{n\text{-}C_{27}}$ =0.22, $R^2_{n\text{-}C_{29}}$ =0.15 and $R^2_{n\text{-}C_{31}}$ =0.27).

Focusing on species-specific correlations between all environmental variables and the $\delta^{13}C$ in n-C_{29}, we have tested *Salicornia australis, Avicennia rensifora, Glossostigma elatinoides, Plantago coronopus* and *Samolus repens* (Figure A.12, A.10, A.11, A.13, A.14 and A.15). Only *Samolus repens* shows significant correlation between the $\delta^{13}C$ in n-C_{29} and salinity.

Data from all species show weak positive correlation between the salinity and $\delta^{13}C$ of n-C_{25}, n-C_{27}, n-C_{29} (Figures 2, A.16 and A.17) and n-C_{31} ($R^2_{n\text{-}C_{25}}$ =0.11, $R^2_{n\text{-}C_{27}}$ =0.13, $R^2_{n\text{-}C_{29}}$ =0.12 and $R^2_{n\text{-}C_{31}}$ =0.19, Table 3). Only 146 samples of 11 species out of 281 samples and 16 species samples include salinity data.

We have examined the phylogenetic tree of all collected species and added means of our variables as the traits to each tip of the tree (Figure A.8). Results of the Abouheif's test show no autocorrelation caused by phylogenetic signal in all cases (Table 3): phylogeny with $\delta^{13}C$ in n-C_{29}, and phylogeny with salinity signal. Therefore, there is no significant phylogenetical signal influencing the relationship between the $\delta^{13}C$ in n-C_{29} and salinity.

Further, we used the phylogenetic generalized least squares model, which corrects for the phylogenetic signal, to test the relationship between the $\delta^{13}C$ in n-C_{29} and the salinity. As the phylogenetic approach requires only one value as a trait per species, we used the mean of $\delta^{13}C$ in n-C_{29} and salinity for each species (n = 16). We did not find any significant linear regression (Table A.5), however, this may be caused simply by using only one value of trait per species. When conducting ordinary least squares model, generalized linear model, linear mixing models or Monte Carlo linear regression simulation on the whole dataset (n = 146), we observe consistently significant, albeit weak, linear relationship (Table A.5, Figure 2).

Figure 2: Relationship between salinity, on x-axis, and the carbon isotopic composition in n-C_{29}, on y-axis, in all species expressed through symbols across five studied color-coded coastal environments. The solid lines describe generalized linear models of the full dataset (purple, slope of 0.027 and R^2 =0.11), and of a reduced dataset (green, slope of 0.039 and R^2 =0.07) using the

interquartile range excluding salinity outliers above $100 \mathrm{dS \cdot m^{-1}}$.

All, recent and fossil isotopic data are normally distributed within the entire dataset, as well as, within separate ecosystem types and species. We have tested the significance of the variance of $\delta^{13}C$ in $n\text{-}C_{29}$ values and salinity using several statistical approaches (Methods section 2.5) resulting in most tests confirming the data to be significantly different between species and types of localities (e.g, t-tests: all p-values $< 2.2 \cdot 10^{-16}$, see additional test in Tables A.6, A.7). From Kolmogorov-Smirnov tests of the variance between the various ecosystems, we observe that the $\delta^{13}C$ in $n\text{-}C_{29}$ values of dunes are not significantly different from the isotopic values of salt marshes, salt marshes transitioning to mangrove and to mangroves (Table A.7). This can be caused by one common factor in all of these environments – osmotic stress. Here drought and salinity cannot be untangled. Additionally, similar test show that mangroves and salt marsh transitioning to mangroves are not significantly different in their isotopic values, but saltmashes have significantly different isotopic signature. This could be caused by the salinity gradient responsable for the vegetation composition in these environments, where mangroves, comprise of better adapted species compared to salt marshes. However, when using ANOVA approach, all environments and species have significantly different $\delta^{13}C$ in $n\text{-}C_{29}$ values.

Therefore, based on the isotopic composition of separate species (Figure 3), which are also characterized by ranges of salinity, the approximate calibration can be used, with caution, for interpretation of the relative salinity stress in fossil environments. Even though there is a weak trend observed between the species gradient based on $\delta^{13}C$ in $n\text{-}C_{29}$ values and the salinity (Figure 3), the data show rather the ability of species to cope with increased salinity stress. As an example, *Plantago coronopus* grows in wide range of salinities, yet the isotopic composition shows relatively lower values. Our control species – *Plantago lanceolota* – growing in low salinity, show relatively lower isotopic, similar to salinity-stressed and/or adapted *P. coronopus* (Figure 3). An exception is *Pittosporum crassifolium*, showing in low salinities relatively higher isotopic signature, which is caused by increased drought as it is classified as a xerophytic plant common in dune forest (Cooper, 1956).

Table 3: Results of Pearson's correlation between salinity and separate *n*-alkanes on all species.

Second part shows the results of Abouheif's test of phylogenetic signal in trait data, in our case salinity and $\delta^{13}C_{n\text{-}C_{29}}$. Obs stands from observed Moran statistics and its standard deviation (STD obs). A positive Moran's value indicates that similar values tend to cluster together, while a negative value indicates that dissimilar values tend to cluster together. A Moran's value of zero indicates that there is no spatial autocorrelation.

Pearson's correlations					
Compound in all species	*n*	R	R^2	p-value	Degrees of freedom (df)
n-C_{25}	225	0.33	0.11	$1.5 \cdot 10^{-4}$	129
n-C_{27}	269	0.37	0.13	$5.8x \cdot 10^{-6}$	144
n-C_{29}	281	0.34	0.12	$2.6x \cdot 10^{-5}$	145
n-C_{31}	221	0.44	0.19	$2.8x \cdot 10^{-8}$	144
Abouheif's test of phylogenetic signal					
		Obs	STD obs	p-value	
Phylogenetic signal effect in salinity		0.0934	1.1291	0.128	
Phylogenetic signal effect in $\delta^{13}C_{n-C_{29}}$		0.0934	1.1157	0.136	

Figure 3: Inset A: Ranges of stable carbon isotope values (0) in *n*-C_{29} of all sampled species sorted from the isotopically relatively lightest to the heaviest. Inset B: Salinity ranges (in dSm^{-1}) of the majority of samples species. The black circles are individual data points with white circles denote median.

When summarizing the $\delta^{13}C$ in *n*-C_{29} of all species according to the environment, from deltaic to mangrove coastal ecosystem, the greatest range is observed in salt marshes (Figure 4). The relatively lightest isotopic signatures are observed in deltaic systems compared to the relatively heaviest signatures in the salt marshes invaded by mangroves transition zones. These results are in an agreement with the effect of increased salinity on the $\delta^{13}C$ (Ladd and Sachs, 2013; He et al., 2021; Park et al., 2019).

Figure 4: Summary violin plots showing ranges of $\delta^{13}C$ in *n*-C_{29} from five different coastal

ecosystems. The black circles are individual data points with white circles denote median.

In addition to the isotopic signatures of n-C_{29}, we have examined patterns in the isotopic composition of all species and all identified *n*-alkanes from length n-C_{16} to n-C_{31} (Figure A.18). Firstly, we have observed a relatively higher abundance of short even *n*-alkanes (n-C_{16} - n-C_{22}) compared to odd. This phenomenon was already observed and explained by combustion processes (Kuhn et al., 2010). These short *n*-alkanes exhibit a relatively heavier isotopic signatures, which corresponds to the mechanism of isotopic discrimination during carbon chain formation (Eglinton and Hamilton, 1967).

3.2. The fossil dataset – cuticular n-alkane $\delta^{13}C$

Similar to the recent plant species, the ranges of the stable carbon isotopic signature $\delta^{13}C$ of the *n*-alkanes measured on fossil plant leaves show high variability. Data of $\delta^{13}C$ in n-C_{29} from all species (n = 83) vary between -22.10 to -39.50 (Figure 5) with an average of -29.80 and median of -29.50. The relatively lightest values are observed for *Cunninghamites lignitum*, which occurs in sediments of Unit 3a and 5. The heaviest $\delta^{13}C$ values are found in *Nilssonia mirovanae*, which was found in sediments of the Unit 1.

Summary of the $\delta^{13}C$ in n-C_{29} of all species according to the units, from deltaic U1 to salt marsh ecosystem in U3b and coastal swamp in U5, shows the greatest range in the salt marsh Unit U3b (Figure 6), which is in agreement with our recent data (Figure 4). The relatively lightest isotopic signatures are observed in fluvial, deltaic and coastal swamp systems, where the osmotic stress is not as high as in the salt marsh, upland and slope mesophytic areas of Unit U3. The highest values are recorded in fossil plants that are (due to their fragmentary nature and micromorphological features) representatives of upland and slope vegetation. Thus, both the recent and the fossil data further suggest the $\delta^{13}C$ in *n*-alkanes reflect the general trend salinity/osmotic stress changes.

The Kolmogorov-Smirnov tests of the variance between the various ecosystems shows that the $\delta^{13}C$ in n-C_{29} values of swamp are not significantly different from the isotopic values of salt marshes (Table A.7). Similarly, the salt marsh isotopic values are not significantly different from

the alluvial plain and slope environment. All of these environment have potential of osmostic stress, in form of salinity (salt marsh, alluvial plain), water-logging (swamp), or drought (alluvial plain and slope). As these osmotic stressors cannot be untangled in the isotopic values, these units do not show statistically significant difference. The results of a variance test (Table A.7), show similar phenomenon of the isotopic values not being able to distingiush various types of osmotic stressors, thus, showing not significant variance between swamp and channel infills (drought - water-logging), as well as, channel infills and salt marsh (water-logging - salinity). However, when using ANOVA approach, all environments and species have significantly different $\delta^{13}C$ in $n\text{-}C_{29}$ values (Table A.6).

In addition to the $\delta^{13}C$ in $n\text{-}C_{29}$, we examined the distribution of $\delta^{13}C$ in all identified alkanes. The expected pattern of relatively heavier short carbon chains and lighter longer alkanes is observed in most of the samples (Figure A.19). However, for some samples, the relative abundances of some *n*-alkenes were below the detection limit, or the amount of full chemical replicates was low and thus, some *n*-alkanes are not present in the record, e.g., *Nilssonia mirovanae, Papillaeophyllum labutae, Pseudoctenis babinensis*. *Ascarinophyllum pecinovense* and *Pseudoasterophyllites cretaceus* show opposite trend in the alkanes, where isotopically heavier values are found in the longer *n*-alkanes. This could be potentially linked to osmotic stress, salinity and drought, however, we don't observe this phenomenon in our modern data. Although cuticles of these samples were showing no preservation issues or diagenetic effect, this pattern in the isotopic data may be linked to preservation. More investigation is needed on the preservation of *n*-alkanes to be more conclusive about the observed phenomenon. For the rest of the samples, similarly to the modern samples *n*-alkane distribution, we do not observe any specific pattern in the $\delta^{13}C$ of all *n*-alkanes which could be indicating osmotic stress.

Figure 5: Ranges of stable carbon isotope values (0) in $n\text{-}C_{29}$ of all sampled fossil species sorted from the isotopically relatively heaviest to the lightest. The black circles are individual data points with white circles denote median.

Figure 6: Summary violin plots showing ranges of $\delta^{13}C$ in $n\text{-}C_{29}$ from five sedimentary units representing different coastal settings Unit 1 (U1) represents fluvial environment, Unit 2 (U2) is

formed in tide-influenced fluvial setting, Unit 3b (U3b) is composed of estuarine march sediments, Unit 3c (U3c) are plants from river slopes or upland and Unit 5 (U5) is coastal swamp (Uličný et al., 1997b). The black circles are individual data points with white circles denote median.

3.3. Patterns in isotopic data of modern coastal environments and relative n-alkanes distribution

We do not aim to quantify the *n*-alkanes; however, the *n*-alkanes relative abundances have a potential to reflect the environmental settings, e.g., conifers show high abundances of long-chained $n\text{-}C_{29}$ to $n\text{-}C_{35}$ alkanes compared to herbs, which have higher relative abundance of $n\text{-}C_{25}$ to $n\text{-}C_{29}$ (Liu et al., 2022; Diefendorf and Freimuth, 2017).

Looking at the *n*-alkane relative distribution and their $\delta^{13}C$ (Figure A.19), no abnormal patterns in the long-chain alkanes were observed, which gives us certainty about quality of our fossil sample preservation. Our data are in an agreement with the common odd-over-even *n*-alkanes distribution (Eglinton and Hamilton, 1967) in the long-chains. During the carbon chain prolongation, every step of carbon addition brings fractionation (Zhou et al., 2010, 2015). Thus, the longer the *n*-alkane carbon chain is, the more is depleted in ^{13}C because of simply more fractionation steps. This pattern combined with the saw-like pattern observed by Zhou et al. (2010) was observed in most of our modern samples and in some of the fossil samples (Figures A.18 and A.19).

Some shorter *n*-alkanes are completely absent in our samples (Figures A.18 and A.19). It was previously suggested that plants growing in higher osmotic stress, e.g. succulents, halophytes and xerophytes, produce longer *n*-alkanes simply as a response to the environmental stressors (Vogts et al., 2009; Schefuß et al., 2003). This may explain why in both, modern and fossil samples, not all species has shorter *n*-alkanes detected/present (Figures A.18 and A.19).

Additionally, when shorter *n*-alkanes are present, they often show even-over-odd pattern which has been previously attributed to (1) the diagenetic reduction of *n*-fatty acids under reducing conditions (e.g., Welte and Ebhardt, 1968) or (2) input from some specific bacteria or fungi (e.g., Davis, 1968; Han and Calvin, 1969; Jones, 1969; Fisher et al., 1972; Tu et al., 2000). However, Kuhn et al. (2010) showed that C3 plants can contain higher quantities of short chain *n*-alkanes of purely biologic origin. Therefore, we do not suspect any diagenetic effects in our samples. We

rather hypothesize that the presence of even-over-odd short *n*-alkanes combined with odd-over-even long *n*-alkanes in the same sample suggest either (1) an exposure of the fossil plant to a fire event, which was not vigorous enough to burn the plant completely (Dettweiler et al., 2003; Wiesenberg et al., 2009) and which could have been part of their quick deposition and preservation process, or (2) inclusion of the marine sediment in the fossil material which is characterizing with shorter chains of algal or phytoplankton origin (Blumer et al., 1971; Meyers and Ishiwatari, 1993).

3.4. Differences between the modern and fossil $\delta^{13}C$

Our fossil data are well fitting into the published Mesozoic $\delta^{13}C_{n-alkane}$ values (Richey et al., 2023), when taking into account that we look at only $\delta^{13}C_{n-C_{29}}$. After the correction for different $\delta^{13}C_{air}$ values, the modern $\Delta^{13}C$ (fractionation) values are ranging between 19.5 to 32.90 with and average value of 25.60. Values for the late Cenomanian vary from 17.5 to 35.90 with and average value of 25.60 (Figure A.9). Thus, we observe a comparable fractionation of the Cretaceous material with the modern $\Delta^{13}C$. This would suggest that our selected modern environments are very much analogous in terms of isotopic fractionation to the Cretaceous.

4. Discussion

4.1. Building an interpretation framework from the modern data

This study aimed to test the relationship between $\delta^{13}C$ values and osmotic stressors in order to support traditional palaeobotanical approaches, e.g., cuticle analysis, of plant habitat reconstruction. Fossil record is limited in preserved information and that is why we examined close to analogous modern environments, where more information can be captured. However, our knowledge on fossil plant physiology will likely remain limited, especially for extinct species.

In conditions of osmotic stress, the plant stomatal conductance is affected due to low leaf water potential (Farquhar and Sharkey, 1982). The plant closes its stomata and thus the ratio of intercellular and ambient partial pressures of CO_2 (c_i/c_a) is changing and causes changes in the stable carbon isotope fractionation (Farquhar et al., 1982). In this case, even the long-chain *n*-alkanes will show systematic shift towards more ^{13}C-enriched values (Eglinton and Hamilton,

1967). For comparing the $\delta^{13}C$ of all plant samples, we have chosen the $n-C_{29}$ alkane as it is found in majority of all plant species (Liu et al., 2022; Diefendorf and Freimuth, 2017).

Building upon our mechanistic model, we investigated the relationship between salinity and $\delta^{13}C$ in our modern dataset. However, the variation in $\delta^{13}C$ could only be partially attributed to salinity (Figure 2, Table 3). This incomplete explanation likely stems from species-specific responses to salinity, interacting with other environmental factors like mean annual precipitation (MAP), mean annual temperature (MAT), and water availability. These factors exhibited variability across study sites, ranging from 800 to 1500 mm for MAP a nd 9 to 16 C for MAT or 12-36 C for annual maximum temperature. Both MAP and MAT influence stomatal conductance, which in turn impacts $\delta^{13}C$ values (e.g., Ceccopieri et al., 2021; Diefendorf et al., 2010; Diefendorf and Freimuth, 2017).

Furthermore, we observed that not all species exhibit a positive or even substantial response to salinity stress (Figure 3). This variation could arise from various factors, including dynamically changing osmotic stress (salinity, drought), water availability, adaptations to extreme environments, such as switching from C3 to CAM metabolism (Winter et al., 2005; Winter and Holtum, 2014), physiological adaptations (e.g., xerophytes and halophytes, Farquhar et al., 1982), or the combined effect of multiple environmental stressors (Farquhar et al., 1989; Arens et al., 2000; Cernusak et al., 2013). Additionally, the species-specific response of isotopic data could be explained by differences in water use efficiency across species (reviewed by Liu et al., 2022).

For our interpretative framework, we follow the literature (Ladd and Sachs, 2013; Neales et al., 1983; Guy et al., 1989; Park et al., 2019; He et al., 2021, 2022) and our results, which still suggest that the $\delta^{13}C_{n\text{-alkanes}}$ values partly reflect the osmotic stress of the plant even if the plant has adaptation to high-salinity or low water availability conditions, such as halophytes or xerophytes.

Looking back to our data, the $\delta^{13}C$ values of most species varies within a reasonable range (-27.4 to -40.10) compared to reviewed C3, likely not osmostically stressed, plants $\delta^{13}C$ mean value of -350 (Liu and An, 2020), which may reflect the presence of tolerance towards the osmotic stress in our dataset. By combining the individual data with the variation between species, variation of different coastal environments (Figure 3, 4 and Table A.7) and the knowledge from the current literature, an approximate interpretative framework can be defined (Figure 7).

Figure 7: A proposed interpretation scheme of $\delta^{13}C$ in n-C_{29} of leaf waxes from sampled coastal environments.

We additionally suggest that species with wider spread of isotopic values are capable to grow in osmotically dynamic environment where, they need to cope with greater changes in osmotic stress such as the seaward/tidal zone (Waycott et al., 2011), e.g., *Avicennia rensifera, Samolus repens, Salicornia australis* (Figure 3). In our modern samples it is *Avicennia rensifera* which has the widest range of $\delta^{13}C$ (Figure 3) and respond to salinity (Figure A.12). *A. rensifera* is a mangrove tree which can cope with very high salinities (e.g., Tomlinson, 1986; Park et al., 2019; He et al., 2021), and thus is capable to grow in very diverse coastal settings. This is confirmed by its successful invasion to the New-Zealand salt marshes (Lundquist et al., 2017). Similarly, species with narrow range are either not able to adapt to osmotic stress or are adapted to a very specific type of osmotic stress, e.g. xerophytic *Pittosporum crassifolium* (Figure 3).

Thus, we attempt to apply our interpretative framework (Figure 7) to already well-studied Cretaceous flora. We combine the $\delta^{13}C$ in n-C_{29} with published cuticular characterization of each studied species (Čepičková and 555 Kvaček, 2022; Čepičková and Kvaček, 2023, in review) and well-studied sedimentology (Uličný et al., 1997b) to have independent proxies for the osmotic stress interpretation as some of the species may be well adapted to salinity.

4.2. Application of the interpretation framework to fossil environments

For majority of the fossil species, we were able to reconstruct the plant habitat. Further, we have summarized all plant species from each unit into violin plots (Figure 6) to support the sedimentological and palynological interpretation of the units by Uličný et al. (1997b). Isotopic values of Unit U1 and U2 agree with the sedimentology and represent the fluvial (deltaic) and tide-influenced fluvial environment (Figure 6). The Unit U3 divided into several subunits indicates different level of water stress (both salinity and drought). Fossil plants coming from the subunit U3b – salt marsh – follows the trend expected for salt marsh environment as it shows relatively higher $\delta^{13}C$ values. This pattern between deltaic and salt marsh units is also seen in the modern data (Figure 4). The samples from U3c – the channel infills bearing mixture of para-autochthonous

and allochthonous fossil plant remains (from slope and upland) show very high-water stress. This could be caused by salinity stress in case of the para-autochtonous plants growing on the slopes of tidal rivers, or drought in case of the upland originating allochtonous plants.

The samples from Unit U3c demonstrate that for individual habitat determination, we still must be aware that the $\delta^{13}C$ in $n\text{-}C_{29}$ can reflect not only salinity stress, but also drought, combined stress or a species-specific response. One good example of potential misinterpretation while using only isotopic data without the cuticular data is *Frenelopsis alata*. Solely based on the isotopic data, we would interpret *F. alata* as a plant growing in an well-watered habitat with no osmotic stresses. However, from the morphological observations (Kvaček, 2000; Gomez et al., 2002), fossil conifer *Frenelopsis alata* is an analogous case in terms of coping strategy (xerophyte) to *Calystegia soldanella*. It is known, that some frenelopsids as *Frenelopsis alata* or *F. turolensis* grew in haline conditions (Kvaček, 2000; Gomez et al., 2002). Other species are interpreted as oligohaline (*F. ugnaensis*, Gomez et al., 2002) or xerophytic (*Frenelopsis ramosissima*) from the Early Cretaceous of USA (Upchurch et al., 1981), *F. antunesii* from the Aptian-Albian of Portugal (Mendes and Kvaček, 2022). There is a hypothesis that the halophytic members of *Frenelopsis* developed from xerophytes (e.g., Mendes and Kvaček, 2022), that were well equipped to cope with water stress. We can observe parallel evolution in modern halophytes having morphological and physiological adaptation to water stress developed from species that were initially xerophytic as it is the case of number of modern halophytic Chenopodiaceae (Grigore and Toma, 2021).

Thus, it is crucial to have additional proxies for the complex environment reconstruction, such as sedimentology, and in our case, also data from cuticle analysis. Combining morphological description and cuticular data by Kvaček (1997, 1999b, 2000, 1999a); Kvaček et al. (2005, 2012, 2006); Čepičková and Kvaček (2022); Čepičková and Kvaček (2023, in review) with our isotopic data we suggest following autecologies: Salt marsh plants and swamps (4.2.1), Upland and river valley slope (4.2.2), Alluvial plains (4.2.3). These autecologies are described in following sections.

4.2.1. Salt marsh plants and swamps – salinity stress and adaptations

Abundant *Frenelopsis alata* described as Cheirolepidiaceae conifer has very thick cuticle, equipped with stomata surrounded by papillae, sunken in deep stomatal pits (Kvaček, 2000). From morphological as well as from the isotopic data, *Frenelopsis* has certainly an adaptation to water stress, which results in relatively light isotopic composition, although it was growing in Unit U3b

– salt marsh sediments containing numerous marine plankton and it is firmly associated with sea-coast tidal system. The wide spread of the isotopic values suggest its capability to cope with great changes in salinity locally on individual plant/specimen level.

Interestingly, add conifers of our dataset – *Frenelopsis alata*, *Cunninghamites lignitum* and *Sphenolepis pecinovensis* show relatively the lightest $\delta^{13}C_{n-C29}$ in our dataset (Figure 5) and are lighter than reported Creataceous conifer data in Richey et al. (2023). All our angiosperms show relatively heavier isotopic values compare to the gymnosperms, which is the very opposite direction of the isotopic shift than reported in the literature (Sheldon et al., 2020; Diefendorf et al., 2010; Diefendorf and Freimuth, 2017; Richey et al., 2023). Therefore, these conifers were either growing in non-osmotically stressing environment or adapted to drought and/or salinity, likely because they grew in zones, were angiosperms showed only limited tolerances to salinities, e.g., the tidal zone.

Accompanying plant species *Eretmophyllum obtusum* – gikgoalean plant – shows obtuse coriaceous leaves with very thick cuticle (Kvaček, 1999a; Čepičková and Kvaček, 2023, in review). Its stomata are surrounded by a rim and are sunken in stomatal pits (Kvaček et al., 2005). This plant is equally frequent as *Frenelopsis alata* in tidal sediments of Unit U3b. It is reconstructed to be a part of salt marsh vegetation (Uličný et al., 1997b; Kvaček et al., 2006). Among the salt marsh halophytes, it shows one of the highest water stress (Figure 5) through relatively heavy isotopic values. The isotopic values are lighter then published (Richey et al., 2023), but this can be explained by using compound specific isotopic values in our dataset, which are generally lighter compared to bulk values. This gingkolean plant follows the expected shift in isotopic values against angiosperms, where gingkoes should have isotopically heavier values (Sheldon et al., 2020; Richey et al., 2023). The salinity stress was likely caused by saline water ingression delivered by tidal channels.

A small herbaceous angiosperm – *Pseudoasterophyllites cretaceus* – has small leaves with thick cuticle (Čepičková and Kvaček, 2023, in review). Its cylindric succulent leaves and robust stamens possess in terminal parts epidermal papillae (Kvaček et al., 2012, 2016). The relatively heavy isotopic values (Figure 5) suggest high salinity stress, which may be explained by its growth in the very saline, often tide-flooded coastal habitats, where other plants cannot grow. This small herbaceous plant was growing in the tidal zone and each individual plant was salinity stressed in different extend, depending on the local exposure to saline water.

"Diospyros" cretacea is an angiosperm reconstructed as shrub or small tree and its leathery entire-margined leaves show very thick cuticle (Čepičková and Kvaček, 2023, in review). It is frequently found in sediments of in-land parts of salt marshes (Uličný et al., 1997b). This is the second angiosperm in the salt marsh vegetation. The isotopic values show quite high and wide spread of water stress, potentially both, salinity and drought (Figure 5). This suggest that *"Diospyros"* foliage represents probably some early angiosperm from ANITA or Chloranthales group, which could cope with wide salinity and drought ranges. It could be potentially one of the species with the coping mechanism of metabolic pathway switch from C3 to CAM under high osmotic stress. Therefore, combining the cuticular data and the isotopic values, these indicate that this plant was growing probably in marginal parts of salt marsh exposed to both, irregular salinity and potential drought stress.

Cunninghamites lignitum is a long leaved conifer bearing large ovuliferous cones (Kvaček, 1999b; Bosma et al., 2012). Its isotopic values show the second largest variation which can be explained by wide range of stressors. When showing very light values, it can be not stressed at all. When exhibiting heavier values, with regard to the sedimentary interpretation of a swamp, this plant could be exposed to no water limitation, but the opposite – water-logging. This behaviour was observed in modern species growing on riverbanks exposed to water-logging (Fan et al., 2018), resulting in heavier isotopic values. Therefore, considering all proxies we support the interpretation that it was growing in coastal swamps (Uličný et al., 1997b; Kvaček et al., 2006) and/or alternatively it was growing on a periodically flooded alluvial plain or riverbanks.

Another conifer, *Sphenolepis pecinovensis* show relatively small water stress, which corresponds with no water limitation. This cupressaceous conifer grew probably together with *C. lignitum* in coastal swamp (Kvaček, 1997; Uličný et al., 1997b). For this conifer the same is valid as stated above for *C. lignitum*.

4.2.2. Upland and river valley slope – drought stress

We also examined a cycad – *Pseudoctenis babinensis* – with pinnately arranged fronds showing thick cuticle and stomata sunken in pits (Kvaček, 2008; Čepičková and Kvaček, 2020). Due to fragmentary nature of the fossil in sediment and cuticle physiognomy, it is considered to be a plant that was growing on slopes or upland (Čepičková and Kvaček, 2020). The $\delta^{13}C$ in $n\text{-}C_{29}$ values suggest that this plant was under serious osmotic stress, or alternatively, it reflect the species-specific fractionation, as it is a cycad. However, the fragmentary material was present only in Unit 1, which is a unit without any marine influence. Thus, this supports that it was growing on upland, in an environment with low water availability.

Similar to *P. babinensis*, another cycad – *Nilssonia mirovanae* – is with pinnately arranged fronds having thick cuticle and stomata surrounded by large papillae (Čepičková and Kvaček, 2020). Again, due to very fragmentary character of the fossil in sediment and its cuticle morphology, this taxon is also considered to be a part of upland and slope of the river valley vegetation (Čepičková and Kvaček, 2020), which is in an agreement with the isotopic values suggesting serious osmotic stress caused by drought.

Both of our cycads show the relatively heaviest isotopic values in our entire dataset (Figure 5). Cycads should show quite similar isotopic values to angiosperms, just slightly heavier (Richey et al., 2023), which is observed in our data. Therefore, we can hypothesize that if our angiosperms are osmotically (both salinity and drought) stressed, these cycads must be also stressed. Thus, their order-specific fractionation may be linked to either adaptation to very dry environments or to an osmotic stress due to no adaptation to drought.

A coriaceous angiosperm leaf of *Papillaephyllum labutae* has thick cuticle and teeth papillae containing resin. Its abaxial cuticle is covered by large papillae (Čepičková and Kvaček, 2023, in review). Due to its extreme cuticle physiognomy, it is considered to grow on upland (Čepičková and Kvaček, 2023, in review). The relatively higher $\delta^{13}C$ in $n\text{-}C_{29}$ values support that this plant grew in dry conditions of the upland with low water availability, thus high drought stress (Figure 5).

4.2.3. Alluvial plains – combination of osmotic stressors and water availability

A coriaceous angiosperm leaf with resin bodies particularly in marginal papillae – *Ascarinophyllum pecinovense* – has epicuticular striations (Čepičková and Kvaček, 2022). This

plant is interpreted to grow on river valley slopes or on bars in alluvial plains (Čepičková and Kvaček, 2022). The wide spread of relatively higher $\delta^{13}C$ values (Figure 5) suggest that these plants were exposed to a combination of stressors depending on the individual level. Some individuals on sand bars or flood plain may have good access to water; however, events of tidal floods or droughts caused by river flow fluctuation could induce both salinity and drought stress.

Lauroid leaves *Myrtophyllum geinitzii* and *Eucalyptolaurus* sp. show medium to thin cuticles (Uličný et al., 1997b). They are associated with reproductive structures *Mauldinia bohemica* and *Pragocladus lauroides* (Eklund and Kvaček, 1998; Kvaček and Eklund, 2003) and are interpreted as major components of alluvial braided river plains. This interpretation is supported by the relatively light isotopic values indicating very mild salinity and drought stress.

Similarly, *Ettingshausenia laevis*, a platanoid foliage with very thin cuticles associated with staminate globular inflorescences *Platananthus* sp. (Kvaček 732 and Eklund, 2003), has relatively light isotopic values suggesting mild or no salinity nor drought stress. These platanoids together with reproductive structure *Ceratoxylon* of unknown affinity are thus interpreted as plants of flood plain vegetation.

Usually preserved in fragments, *Araliaephyllum* sp. has medium thick cuticle (Kvaček, 1992). Its isotopic values suggest no or very mild salinity and drought stress and thus, it is interpreted as growing in higher parts of alluvial plains and slopes with a good freshwater availability.

4.3. Overall palaeorecostruction evaluation

In general, plants that are less or not at all stressed are from azonal vegetation growing in flood plains and coastal, and back swamps being constantly or periodically water supplied by river systems – e.g., *Eucalyptolaurus* sp., *Ettingshausenia laevis*, (from fluvial U2) and conifers *Cunninghamites lignitum* and *Sphenolepis pecinovensis* (from swampy U5). The salt marsh and mangrove-like habitats are occupied by species which can cope with increased salinities, e.g., conifer *Frenelopsis alata*, but many of them are still showing some response on the salinity stress in the $\delta^{13}C$ – *Eretmophyllum obtusum, Pseudoasterophyllites cretaceus* and *Diospyros cretacea*.

Worth noticing is the fact, that conifers group together in the very lightest isotopic values, which is not expected, based on the published differences in plant groups. According to the literature (reviewed in Richey et al., 2023; Sheldon et al., 2020; Hare and Lavergne, 2021), it is

suggested that angiosperms should have relatively the lightest $\delta^{13}C$, followed by cycads, ginkgoes and the heaviest values should be found in conifers. In our dataset, conifers and ginkgoes do not follow this trend, as they show the lightest values. This could be potentially explained by variable MAP, MAT and CO_2 concentration, where gymnosperms were shown to exert little response on these variable (Sheldon et al., 2020; Hare and Lavergne, 2021), whereas angiosperms do respond. Thus, potentially the higher sensitivity to environmental changes are rather reflected in our angiosperm data then in the conifers. Gymnosperms would likely reflect daytime vapour pressure deficit (changes in air moisture) (Hare and Lavergne, 2021).

Similarly, cycads group together, however, they do follow the expected isotopic signature/fractionation cascade. Therefore, their relatively the heaviest isotopic values of our dataset may be linked to order-specific fractionation – either thorough adaptation to very dry environments or the ability to switch from C3 to CAM metabolism, which we also hypothesize for some angiosperms.

4.4. Limitations of the study and outlook

We have identified several limitation of our study which may have improved the understanding of the response of $\delta^{13}C_{n\text{-alkanes}}$ to osmotic stress. Firstly, as discussed, there is a great uncertainty for the interpretation of the isotopic values of fossil species due to the potential species-specific fractionation demonstrated on the modern species (Ladd and Sachs, 2013; Park et al., 2019; He et al., 2021). Linked to this, it is hard to constrain whether species can be able to switch their metabolism from C3 to CAM in the past, similarly to the documented modern plant species (Winter et al., 2005; Winter and Holtum, 2014). We still need better understanding of modern plant photosynthetic pathways fluidity.

Further, our recent dataset is collected from various geographical location with different MAP and MAT. Therefore, the modern calibration can be biased by the effect of MAP and MAT as it was shown previously in the literature to have a substantial effect on the isotopic values (e.g., Kuhn et al., 2010; Diefendorf et al., 2010; Diefendorf and Freimuth, 2017; Ceccopieri et al., 2021,, and many more). Additionally, the concentration CO_2 ($[CO_2]$) and the atmospheric $\delta^{13}C_{air}$ (carbon source) is also affecting the isotopic resulting signature (Farquhar et al., 1989). With a variable $[CO_2]$ and $\delta^{13}C_{air}$ thought the Mesozoic (Barral et al., 2017), the comparison of the

modern data and fossil data may be biased. A correction has been applied, but in our case, we have only one value for the entire late Cretaceous. Therefore, we cannot constrain the effect of the temporal $\delta^{13}C_{air}$ variation in the studied time interval. This can thus bring a bias into our isotopic data and potentially their interpretation.

All of these variables in the fossil record are assumed to be constant, simply due to the different time resolution. If, in the future, there is a higher temporary resolution of the variation of MAP, MAT and $\delta^{13}C_{air}$ for this or any close/analogous fossil locality, we could potentially evaluate whether the isotopic signal is driven by osmotic stress or also by MAT, MAP or $\delta^{13}C_{air}$.

Lastly, even though we target exceptionally well preserved fossil samples, based on the cuticular analysis, there is always an uncertainty in the biomolecules preservation. We did not constrain the potential diagenetic effect nor maturity of the fossil material. Moreover, we did not quantify the biomolecules, which limits our data interpretation and placing our data in wider ecological context, where average carbon chain length (ACL) index or carbon preference index (CPI) is used in paleoecology and chemotaxonomy (e.g., Bush and McInerney, 2013). Our study is thus based on the assumption of exceptionally good preservation of the fossil material.

5. Conclusions

We build a data set from modern coastal environments by collecting plant leaves in salt marshes, mangroves, coastal dunes, river deltas and salt marshes invaded by mangroves. We have analysed the plant leaves for their leaf waxes by extraction and measuring stable carbon isotopes in *n*-alkanes and tested the relationship between $\delta^{13}C_{n\text{-alkanes}}$ and salinity.

This modern-species dataset used to build an interpretation frame of $\delta^{13}C_{n\text{-alkanes}}$ from coastal ecosystems applied on the Cenomanian upland and coastal flora from locality Pecínov (Czechia) to support the palaeobotanical vegetation reconstruction (based on micromorphology of cuticles) and complete it with plant habitat data comprised of relative osmotic stress of these individual plant specimens.

The main findings of this study are:

1. There is a significant, albeit weak, positive correlation between the $\delta^{13}C_{n\text{-alkanes}}$ of modern C3 coastal plants and salinity. However, the observed correlation is weaker than expected

likely due to adaptations of some species to high osmotic stress, species-specific response or other environmental factors (potentially MAP, MAT and water availability).

2. Successful species growing in wide range of salinities, e.g., *Salicornia* sp. or *Avicennia* sp., show wide ranges of isotopic values which reflects their flexibility to adapt to dynamically changing osmotic stress (both salinity and drought). Thus, species with wider spread of isotopic values are more adaptive compared to species with narrow range of $\delta^{13}C_{n\text{-alkanes}}$.
3. Grouping individual samples into species categories reflects better the species tolerance or intolerance to osmotic stress. On this level, the knowledge form modern data can be applied for interpreting fossil data.
4. We have observed significant differences in isotopic ranges of separate ecosystem. This could be potentially used as "fingerprinting" of coastal ecosystems.

These findings suggest that this non-destructive method of extracting *n*-alkanes from fossil plant leaves provides us with an important local environmental information and the sample can be still used for traditional morphological description and further observations. However, our data also shed light on the limits of using $\delta^{13}C$ values from plant material for climate reconstruction as osmotic stress is notably affecting the isotopic values as shown in previous literature (Arens et al., 2000; Ladd and Sachs, 2013; Park et al., 2019).

6. Acknowledgements

The authors thank Allister Gilbert for helpful advice on sampling sites and for providing literature on New Zealand's coastal flora. Further, the authors thank Jaromír Váňa (National Museum Prague, Czech Republic), Mr. Kadner and Mr. Kejla (České lupkové závody a.s.) for their help during the field excavations in Pecínov quarry. PZ was funded by The Charles University Grant Agency (GA UK), project No. 40217 and supported by UNCE Center for Geosphere Dynamics, UNCE/SCI/006. JK and JČ were supported by a grant from the Czech Science Foundation (project No. 20-06134S).

References

Abouheif, E., 1999. A method for testing the assumption of phylogenetic independence in comparative data. Evolutionary Ecology Research 1, 895–909.

Arens, N.C., Jahren, A.H., Amundson, R., 2000. Can C3 plants faithfully record the carbon isotopic composition of atmospheric carbon dioxide? Paleobiology 26, 173–164. doi: 10.1666/0094-8373(2000)026<0137:ccpfrt>2.0.co;2.

Badewien, T., Vogts, A., Rullkötter, J., 2015. *n*-Alkane distribution and carbon stable isotope composition in leaf waxes of C3 and C4 plants from Angola. Organic Geochemistry 89-90, 71–79. doi: 10.1016/j.orggeochem.2015.09.002.

Barral, A., Gomez, B., Legendre, S., Lécuyer, C., 2017. Evolution of the carbon isotope composition of atmospheric co2 throughout the cretaceous. Palaeogeography, Palaeoclimatology, Palaeoecology 471, 40–47. doi: 10.1016/j.palaeo.2017.01.034.

Blumer, M., Guillard, R., Chase, T., 1971. Hydrocarbons of marine phytoplankton. Marine Biology 8, 183–189. doi: 10.1007/bf00355214.

Bocherens, H., Friis, E.M., Mariotti, A., Pedersen, K.R., 1993. Carbon isotopic abundances in Mesozoic and Cenozoic fossil plants: Palaeoecological implications. Lethaia 26, 347–358. doi: 10.1111/j.1502-3931.1993.tb01541.x.

Bosma, H.F., Kunzmann, L., Kvaček, J., van Konijnenburg-van Cittert, J.H., 2012. Revision of the genus Cunninghamites (fossil conifers), with special reference to nomenclature, taxonomy and geological age. Review of Palaeobotany and Palynology 182, 20–31. doi: 10.1016/j.revpalbo.2012.06.004.

Bush, R.T., McInerney, F.A., 2013. Leaf wax *n*-alkane distributions in and across modern plants: Implications for paleoecology and chemotaxonomy. Geochimica et Cosmochimica Acta 117, 161–179. doi: 10.1016/j.gca.2013.04.016.

CastaÃ±eda, I.S., Schouten, S., 2011. A review of molecular organic proxies for examining modern and ancient lacustrine environments. Quaternary Science Reviews 30, 2851–2891. doi: 10.1016/j.quascirev.2011.07.009.

Ceccopieri, M., Scofield, A.L., Almeida, L., Araújo, M.P., Hamacher, C., Farias, C.O., Soares, M.L., Carreira, R.S., Wagener, A.L., 2021. Carbon isotopic composition of leaf wax n-alkanes in mangrove plants along a latitudinal gradient in brazil. Organic Geochemistry 161, 104299. doi: 10.1016/j.orggeochem.2021.104299.

Čech, S., 2011. Palaeogeography and stratigraphy of the Bohemian Cretaceous Basin (Czech Republic) – an overview. Geologické výzkumy na Moravě a ve Slezsku 18. URL:

https://journals.muni.cz/index.php/gvms/article/download/1676/1312.

Čepičková, J., Kvaček, J., 2020. Two cycads *Nilssonia mirovanae* sp. nov. and *Pseudoctenis babinensis* J. Kvaček from the Cenomanian of the Bohemian Cretaceous Basin (the Czech Republic) as indicators of water stress in the palaeoenvironment. Fossil Imprint 76, 315–324. doi: 10.37520/fi.2020.025.

Čepičková, J., Kvaček, J., 2022. Fossil leaves of Cenomanian basal angiosperms from the Peruc-Korycany Formation, Czechia, central Europe. Review of Palaeobotany and Palynology 309, 104802. doi: 10.1016/j.revpalbo.2022.104802.

Cernusak, L.A., Ubierna, N., Winter, K., Holtum, J.A.M., Marshall, J.D., Farquhar, G.D., 2013. Environmental and physiological determinants of carbon isotope discrimination in terrestrial plants. New Phytologist 200, 950–965. doi: 10.1111/nph.12423.

Coiffard, C., Gomez, B., Kvaček, J., Thevenard, F., 2006. Early Angiosperm Ecology: Evidence from the Albian-Cenomanian of Europe. Annals of Botany 98, 495–502. doi: 10.1093/aob/mcl125.

Cooper, R.C., 1956. The Australian and New Zealand Species of Pittosporum. Annals of the Missouri Botanical Garden 43, 87–188. doi: 10.2307/2394673.

Cranwell, P., Eglinton, G., Robinson, N., 1987. Lipids of aquatic organisms as potential contributors to lacustrine sediments – II. Organic Geochemistry 11, 513–527. doi: 10.1016/0146-6380(87)90007-6.

Davis, J., 1968. Paraffinic hydrocarbons in the sulfate-reducing bacterium *Desulfovibrio desulfuricans*. Chemical Geology 3, 155–160. doi: 10.1016/0009-2541(68)90007-7.

Dawson, T.E., Mambelli, S., Plamboeck, A.H., Templer, P.H., Tu, K.P., 2002. Stable Isotopes in Plant Ecology. Annual review of ecology and systematics 33, 507–559. doi: 10.1146/annurev.ecolsys.33.020602.095451.

Dettweiler, C., Knicker, H., González-Vila, F.J., Almendros Martn, G., Zancada Fernández, M.C., 2003. Monitoring the fire impacts on soil through chromatographic analysis of the lipid fraction, in: Proceedings of the 3rd Scientific Meeting of the Spanish Society of Chromatography and Related Techniques, Artes GráficasGutenburg, Universidad de Almera. p. 149. URL: http://hdl.handle.net/10261/55164.

Diefendorf, A.F., Freimuth, E.J., 2017. Extracting the most from terrestrial plant-derived *n*-alkyl lipids and their carbon isotopes from the sedimentary record: A review. Organic Geochemistry 103, 1–21. doi: 10.1016/j.orggeochem.2016.10.016.

Diefendorf, A.F., Mueller, K.E., Wing, S.L., Koch, P.L., Freeman, K.H., 2010. Global patterns in leaf ^{13}C discrimination and implications for studies of past and future climate. Proceedings of the National Academy of Sciences 107, 5738–5743. doi: 10.1073/pnas.0910513107.

Eglinton, G., Hamilton, R.J., 1967. Leaf Epicuticular Waxes. Science 156, 1322–1335. doi: 10.1126/science.156.3780.1322.

Eglinton, G., Logan, G.A., Ambler, R.P., Boon, J.J., Perizonius, W.R.K., Eglinton, G., Curry, G.B., 1991. Molecular preservation. Philosophical Transactions of the Royal Society of London. Series B: Biological Sciences 333, 315–328. doi: 10.1098/rstb.1991.0081.

Eklund, H., Kvaček, J., 1998. Lauraceous inflorescences and flowers from the Cenomanian of Bohemia (Czech Republic, central Europe). International Journal of Plant Sciences 159, 668–686. doi: 10.1086/297585.

Eley, Y., Dawson, L., Black, S., Andrews, J., Pedentchouk, N., 2014. Understanding of ^{2}H/^{1}H systematics of leaf wax *n*-alkanes in coastal plants at Stiffkey saltmarsh, Norfolk, UK. Geochimica et Cosmochimica Acta 128, 13–28. doi: 10.1016/j.gca.2013.11.045.

Eley, Y., Dawson, L., Pedentchouk, N., 2016. Investigating the carbon isotope composition and leaf wax *n*-alkane concentration of C3 and C4 plants in Stiffkey saltmarsh, Norfolk, UK. Organic Geochemistry 96, 28–42. doi: 10.1016/j.orggeochem.2016.03.005.

Eley, Y., White, J., Dawson, L., Hren, M., Pedentchouk, N., 2018. Variation in Hydrogen Isotope Composition Among Salt Marsh Plant Organic Compounds Highlights Biochemical Mechanisms Controlling Biosynthetic Fractionation. Journal of Geophysical Research: Biogeosciences 123, 2645–2660. doi: 10.1029/2018JG004403.

Falcon-Lang, H.J., Kvaček, J., Uličný, D., 2001. Fire-prone plant communities and palaeoclimate of a Late Cretaceous fluvial to estuarine environment, Pecnov quarry, Czech Republic. Geological magazine 138, 563–576. doi: 10.1017/s0016756801005714.

Fan, R., Morozumi, T., Maximov, T.C., Sugimoto, A., 2018. Effect of floods on the δ^{13}C values in plant leaves: a study of willows in Northeastern Siberia. PeerJ 6, e5374. doi: 10.7717/peerj.5374.

Farquhar, G.D., Ball, M., von Caemmerer, S., Roksandic, Z., 1982. Effect of salinity and humidity on δ^{13}C value of halophytes – evidence for diffusional isotope fractionation determined by the ratio of intercellular/atmospheric partial pressure of CO_2 under different environmental conditions. Oecologia 52 52, 121–124. doi: 10.1007/BF00349020.

Farquhar, G.D., Ehleringer, J.R., Hubick, K.T., 1989. Carbon Isotope Discrimination and Photosynthesis. Annual Review of Plant Physiology and Plant Molecular Biology 40, 503–537. doi: 10.1146/annurev.pp.40.060189.002443.

Farquhar, G.D., Sharkey, T.D., 1982. Stomatal conductance and photosynthesis. Annual review of plant physiology 33, 317–345. doi: 10.1146/annurev.pp.33.060182.001533.

Ficken, K., Li, B., Swain, D., Eglinton, G., 2000. An *n*-alkane proxy for the sedimentary input of submerged/floating freshwater aquatic macrophytes. Organic Geochemistry 31, 745–749. doi: 10.1016/S0146-6380(00)00081-4.

Fisher, D., Holloway, P., Richmond, D., 1972. Fatty acid and hydrocarbon constituents of the surface and wall lipids of some fungal spores. Microbiology 72, 71–78. doi: 10.1099/00221287-72-1-71.

Gomez, B., Martin-Closas, C., Barale, G., de porta, N.S., Thevenard, F., Guignard, G., 2002. Frenelopsis (Coniferales: Cheirolepidiaceae) and related male organ genera from the Lower Cretaceous of Spain. Palaeontology 45, 997–1036. doi: 10.1111/1475-4983.00273.

GreguÅ¡, J., Kvaček, J., Sakala, J., 2020. Charcoalified homoxylous woods from the Cenomanian of the Bohemian Cretaceous Basin (Czech Republic). Review of Palaeobotany and Palynology 282, 104311. doi: 10.1016/j.revpalbo.2020.104311.

Grigore, M.N., Toma, C., 2021. Morphological and anatomical adaptations of halophytes: A review. Springer. doi: 10.1007/978-3-030-57635-6_37.

Guy, R.D., Warne, P.G., Reid, D.M., 1989. Stable Carbon Isotope Ratio as an Index of Water-Use Efficiency in C3 Halophytes – Possible Relationship to Strategies for Osmotic Adjustment, in: Rundel, P.W., Ehleringer, J.R., Nagy, K.A. (Eds.), Stable Isotopes in Ecological

Research, Springer New York. pp. 55–75. doi: 10.1007/978-1-4612-3498-2_4.

Han, J., Calvin, M., 1969. Hydrocarbon distribution of algae and bacteria, and microbiological activity in sediments. Proceedings of the National Academy of Sciences 64, 436–443. doi: 10.1073/pnas.64.2.436.

Hardie, M., Doyle, R., 2012. Measuring Soil Salinity, in: Plant Salt Tolerance. Humana Press, pp. 415–425. doi: 10.1007/978-1-61779-986-0_28.

Hare, V.J., Lavergne, A., 2021. Differences in carbon isotope discrimination between angiosperm and gymnosperm woody plants, and their geological significance. Geochimica et Cosmochimica Acta 300, 215–230. doi: 10.1016/j.gca.2021.02.029.

He, D., Nemiah Ladd, S., Park, J., Sachs, J.P., Simoneit, B.R., Smoak, J.M., Jaffé, R., 2022. Carbon and hydrogen isotopes of taraxerol in mangrove leaves and sediment cores: Implications for paleo-reconstructions. Geochimica et Cosmochimica Acta 324, 262–279. doi: 10.1016/j.gca.2022.02.018.

He, D., Rivera-Monroy, V.H., Jaffé, R., Zhao, X., 2021. Mangrove leaf species-specific isotopic signatures along a salinity and phosphorus soil fertility gradients in a subtropical estuary. Estuarine, Coastal and Shelf Science 248, 106768. doi: 10.1016/j.ecss.2020.106768.

Herman, A.B., Spicer, R.A., Kvaček, J., 2002. Late Cretaceous climate of Eurasia and Alaska: a quantitative palaeobotanical approach. Wien: Ã–sterreichische Akademie der Wissenschaften Schriftenreihe der Erdwissenschaftlichen Kommissionen 15. p. 93–108. URL: https://opac.geologie.ac.at/ais312/dokumente/SchriftR_Erdw_Komm_15_93_108.pdf.

Jombart, T., Balloux, F., Dray, S., 2010. adephylo: new tools for investigating the phylogenetic signal in biological traits. Bioinformatics 26, 1907–1909. URL: https://doi.org/10.1093/bioinformatics/btq292, doi: 10.1093/bioinformatics/btq292, arXiv:https://academic.oup.com/bioinformatics/article-pdf/26/15/1907/48854154/bioinformatics_26_15_1907.pdf.

Jones, J., 1969. Studies on lipids of soil micro-organisms with particular reference to hydrocarbons. Microbiology 59, 145–152. doi: 10.1099/00221287-59-2-145.

Kohn, M.J., 2010. Carbon isotope compositions of terrestrial C3 plants as indicators of (paleo)ecology and (paleo)climate. Proceedings of the National Academy of Sciences 107, 19691–19695. doi: 10.1073/pnas.1004933107.

Kuhn, T.K., Krull, E.S., Bowater, A., Grice, K., Gleixner, G., 2010. The occurrence of short chain *n*-alkanes with an even over odd predominance in higher plants and soils. Organic Geochemistry 41, 88–95. doi: 10.1016/j.orggeochem.2009.08.003.

Kvaček, J., 1992. Leaf and fruit compressions from the Bohemian Cenomanian. Paleovegetational Development in Europe and Regions Relevant to its Palaeofloristic Evolution, 301–305.

Kvaček, J., 1997. *Sphenolepis pecinovensis* sp. nov. a new taxodiaceous conifer from the Bohemian Cenomanian. Mededeelingen van's Rijks Geologischen Dienst. Haarlem 58, 121–128.

Kvaček, J., 1999a. New data and revision of three gymnosperms from the Cenomanian of Bohemia – *Sagenopteris variabilis* (Velenovský) Velenovský, *Mesenea bohemica* (Corda) comb. n. and *Eretmophyllum obtusum* (Velenovský) comb. n. Acta Musei Nationalis Pragae, Series B, Historia Naturalis 55, 15–24.

Kvaček, J., 1999b. Two conifers (Taxodiaceae) of the Bohemian Cenomanian (Czech Republic, Central Europe). Acta Palaeobotanica 2, 129–151. URL: https://www.researchgate.net/profile/Jiri-Kvacek/publication/259536865_Two_conifers_Taxodiaceae_of_the_Bohemian_Cenomanian_Czech_Republic_Central_Europe/links/0c96052c6dbb1b8a21000000/Two-conifers-Taxodiaceae-of-the-Bohemian-Cenomanian-Czech-Republic-Central-Europe.pdf.

Kvaček, J., 2000. *Frenelopsis alata* and its microsporangiate and ovuliferous reproductive structures from the Cenomanian of Bohemia (Czech Republic, Central Europe). Review of Palaeobotany and Palynology 112, 51–78. doi: 10.1016/s0034-6667(00)00035-x.

Kvaček, J., 2008. New cycad foliage of *Pseudoctenis babinensis* from the Bohemian Cenomanian. Acta Musei Nationalis Pragae, Series B–Historia Naturalis 64, 125–131. URL: https://publikace.nm.cz/en/file/ecec7dbefd837478a9081a28bd122236/16067/sbornik_B_1_08_j_kvacek_screen.pdf.

Kvaček, J., Dašková, J., Renáta, P., 2006. A new schizaeaceous fern, *Schizaeopsis ekrtii* sp. nov.,

and its in situ spores from the Upper Cretaceous (Cenomanian) of the Czech Republic. Review of Palaeobotany and Palynology 140, 51–60. doi: 10.1016/j.revpalbo.2006.02.003.

Kvaček, J., Doyle, J.A., Endress, P.K., Daviero-Gomez, V., Gomez, B., Tekleva, M., 2016. *Pseudoasterophyllites cretaceus* from the Cenomanian (Cretaceous) of the Czech Republic: A possible link between Chloranthaceae and Ceratophyllum. Taxon 65, 1345–1373. doi: 10.12705/656.8.

Kvaček, J., Eklund, H., 2003. A Report on Newly Recovered Reproductive Structures from the Cenomanian of Bohemia (Central Europe). International Journal of Plant Sciences 164, 1021–1039. doi: 10.1086/378824.

Kvaček, J., Falcon-Lang, H.J., Dašková, J., 2005. A new Late Cretaceous ginkgoalean reproductive structure Nehvizdyella gen. nov. from the Czech Republic and its whole-plant reconstruction. American Journal of Botany 92, 1958–1969. doi: 10.3732/ajb.92.12.1958.

Kvaček, J., Gomez, B., Zetter, R., 2012. The Early Angiosperm Pseudoasterophyllites cretaceus from Albian—Cenomanian of Czech Republic and France Revisited. Acta Palaeontologica Polonica 57, 437–443. doi: 10.4202/app.2009.0060.

Kvaček, J., Spicer, R., Herman, A., 2002. Palaeoclimatic parameters based on the Peruc Korycany Flora and its relationship to other Laurasian Cenomanian floras. Moscow: GEOS. p. 164–165.

Kvaček, J., Uličný, D., Svobodová, M., Špičáková, L., 2006. Cretaceous of Central Bohemia. National Museum. p. 58–65.

Ladd, S.N., Sachs, J.P., 2013. Positive correlation between salinity and *n*-alkane δ^{13}C values in the mangrove *Avicennia marina*. Organic Geochemistry 64, 1–8. doi: 10.1016/j.orggeochem.2013.08.011.

Liu, J., An, Z., 2020. Leaf wax *n*-alkane carbon isotope values vary among major terrestrial plant groups: Different responses to precipitation amount and temperature, and implications for paleoenvironmental reconstruction. Earth-Science Reviews 202, 103081. doi: 10.1016/j.earscirev.2020.103081.

Liu, J., Zhao, J., He, D., Huang, X., Jiang, C., Yan, H., Lin, G., An, Z., 2022. Effects of plant types on terrestrial leaf wax long-chain *n*-alkane biomarkers: Implications and paleoapplications.

Earth-Science Reviews 235, 104248. doi: 10.1016/j.earscirev.2022.104248.

Liu, X., Feakins, S.J., Dong, X., Xue, Q., Han, J., Marek, T., Leskovar, D.I., Neely, C.B., Ibrahim, A.M.H., 2019. Evaluating Leaf Wax and Bulk Leaf Carbon Isotope Surrogates for Water Use Efficiency and Grain Yield in Winter Wheat. Crop Science 59, 718–732. doi: 10.2135/cropsci2018.07.0452.

Lundquist, C., Carter, K., Hailes, S.F., Bulmer, R., 2017. Guidelines for managing mangrove (Mānawa) expansion in New Zealand. NIWA. URL: https://docs.niwa.co.nz/library/public/NIWAis85.pdf.

McInerney, F.A., Strömberg, C.A., White, J.W., 2011. The Neogene transition from C3 to C4 grasslands in North America: stable carbon isotope ratios of fossil phytoliths. Paleobiology 37, 23–49. doi: 10.1666/09068.1.

Mendes, M.M., Kvaček, J., 2022. *Frenelopsis antunesii* sp. nov., a new cheirolepidiaceous conifer from the Lower Cretaceous of Figueira da Foz Formation in western Portugal. Review of Palaeobotany and Palynology 300, 104643. doi: 10.1016/j.revpalbo.2022.104643.

Meyers, P.A., Ishiwatari, R., 1993. Lacustrine organic geochemistry – an overview of indicators of organic matter sources and diagenesis in lake sediments. Organic Geochemistry 20, 867–900. doi: 10.1016/0146-6380(93)90100-P.

Neales, T., Fraser, M., Roksandic, Z., 1983. Carbon Isotope Composition of the Halophyte *Disphyma clavellatum* (Haw.) Chinnock (Aizoaceae), as Affected by Salinity. Functional Plant Biology 10, 437–444. doi: 10.1071/pp9830437.

Park, J., Ladd, S.N., Sachs, J.P., 2019. Hydrogen and carbon isotope responses to salinity in greenhouse-cultivated mangroves. Organic Geochemistry 132, 23–36. doi: 10.1016/j.orggeochem.2019.03.001.

Pavoine, S., Ollier, S., Pontier, D., Chessel, D., 2008. Testing for phylogenetic signalin life history variable: Abouheif's test revisited. Theoretical Population Biology 73, 79–91. doi: 10.1016/j.tpb.2007.10.001.

Peters, K.E., Peters, K.E., Walters, C.C., Moldowan, J., 2005. The biomarker guide. volume 1. Cambridge university press. doi: 10.1017/cbo9781107326040.

Rao, Z., Guo, W., Cao, J., Shi, F., Jiang, H., Li, C., 2017. Relationship between the stable carbon isotopic composition of modern plants and surface soils and climate: A global review.

Earth-Science Reviews 165, 110–119. doi: 10.1016/j.earscirev.2016.12.007.

Rayment, G., Higginson, F.R., et al., 1992. Australian laboratory handbook of soil and water chemical methods. Inkata Press Pty Ltd.

Richey, J.D., Nordt, L., White, J.D., Breecker, D.O., 2023. Isoorg23: An updated compilation of stable carbon isotope data of terrestrial organic materials for the cenozoic and mesozoic. Earth-Science Reviews 241, 104439. doi: 10.1016/j.earscirev.2023.104439.

Sachse, D., Billault, I., Bowen, G.J., Chikaraishi, Y., Dawson, T.E., Feakins, S.J., Freeman, K.H., Magill, C.R., McInerney, F.A., van der Meer, M.T., Polissar, P., Robins, R.J., Sachs, J.P., Schmidt, H.L., Sessions, A.L., White, J.W., West, J.B., Kahmen, A., 2012. Molecular Paleohydrology: Interpreting the Hydrogen-Isotopic Composition of Lipid Biomarkers from Photosynthesizing Organisms. Annual Review of Earth and Planetary Sciences 40, 221–249. doi: 10.1146/annurev-earth-042711-105535.

Sage, R.F., 2004. The evolution of C4 photosynthesis. New Phytologist 161, 341–370. doi: 10.1111/j.1469-8137.2004.00974.x.

SchefuÃŸ, E., Ratmeyer, V., Stuut, J.B.W., Jansen, J., Sinninghe Damsté, J.S., 2003. Carbon isotope analyses of *n*-alkanes in dust from the lower atmosphere over the central eastern Atlantic. Geochimica et Cosmochimica Acta 67, 1757–1767. doi: 10.1016/S0016-7037(02)01414-X.

Sheldon, N.D., Smith, S.Y., Stein, R., Ng, M., 2020. Carbon isotope ecology of gymnosperms and implications for paleoclimatic and paleoecological studies. Global and Planetary Change 184, 103060. doi: 10.1016/j.gloplacha.2019.103060.

Tomlinson, P.B., 1986. The Botany of Mangroves. Cambridge University Press. doi: 10.1017/cbo9781139946575.

Tu, T.T.N., Derenne, S., Largeau, C., Mariotti, A., Bocherens, H., Pons, D., 2000. Effects of fungal infection on lipid extract composition of higher plant remains: comparison of shoots of a Cenomanian conifer, uninfected and infected by extinct fungi. Organic Geochemistry 31, 1743–1754. doi: 10.1016/s0146-6380(00)00077-2.

Tu, T.T.N., Kürschner, W.M., Schouten, S., Bergen, P.F.V., 2004. Leaf carbon isotope composition of fossil and extant oaks grown under differing atmospheric CO_2 levels. Palaeogeography, Palaeoclimatology, Palaeoecology 212, 199–213. doi: 10.1016/j.palaeo.2004.05.023.

Uličný, D., Hladíková, J., Attrep, Jr., M.J., Čech, S., Hradecká, L., Svobodová, M., 1997a. Sea-level change and geochemical anomalies across the Cenomanian-Turonian boundary: Pecínov quarry, Bohemia. Palaeogeography, Palaeoclimatology, Palaeoecology 132, 265–285. doi: 10.1016/s0031-0182(97)00055-2.

Uličný, D., Kvaček, J., Svobodová, M., Špičáková, L., 1997b. High-frequency sea-level fluctuations and plant habitats in Cenomanian fluvial to estuarine succession: Pecínov quarry, Bohemia. Palaeogeography, Palaeoclimatology, Palaeoecology 136, 165–197. doi: 10.1016/s0031-0182(97)00033-3.

Uličný, D., Špičáková, L., 1996. Response to high frequency sea-level change in a fluvial to estuarine succession: Cenomanian palaeovalley fill, Bohemian Cretaceous Basin. Geological Society, London, Special Publications 104, 247–268. doi: 10.1144/gsl.sp.1996.104.01.15.

Uličný, D., Špičáková, L., Grygar, R., Svobodová, M., Čech, S., Laurin, J., 2009. Palaeodrainage systems at the basal unconformity of the Bohemian Cretaceous Basin: roles of inherited fault systems and basement lithology during the onset of basin filling. Bulletin of Geosciences 84, 577–610. doi: 10.3140/bull.geosci.1128.

Uličný, D., Kvaček, J., Špičáková, L., Svobodová, M., Čech, S., Hradecká, L., Hladíková, J., Laurin, J., 1996. Pecínov quarry: the record of mid-Cenomanian through early Turonian sea-level changes and related events, in: Fifth International Cretaceous Symposium and Second Workshop on Inoceramids, Stratigraphy and facial development of the Bohemian-Saxonian Cretaceous basin, pp. 1–15.

Upchurch, G.R., Doyle, J.A., Romans, R., 1981. Paleoecology of the conifers Frenelopsis and Pseudofrenelopsis (Cheirolepidiaceae) from the Cretaceous Potomac Group of Maryland and Virginia. Geobotany II 167, 202. doi: 10.1007/978-1-4899-4989-9_8.

Valdes, P., Sellwood, B., Price, G., 1996. Evaluating concepts of Cretaceous equability. Palaeoclimates 2, 139–158.

Vogts, A., Moossen, H., Rommerskirchen, F., Rullkötter, J., 2009. Distribution patterns and stable carbon isotopic composition of alkanes and alkan-1-ols from plant waxes of African rain forest and savanna C3 species. Organic Geochemistry 40, 1037–1054. doi: 10.1016/j.orggeochem.2009.07.011.

Wang, J., Sun, P., Bai, Y., Liu, Z., Cheng, R., Li, Y., 2022. Carbon isotopes of *n*-alkanes allow for

estimation of the CO_2 pressure in the Early Jurassic – A case study from lacustrine shale and cannel boghead in the Dachanggou Basin, Xinjiang, Northwest China. Palaeogeography, Palaeoclimatology, Palaeoecology 607, 111252. doi: 10.1016/j.palaeo.2022.111252.

Wang, J., Xu, Y., Zhou, L., Shi, M., Axia, E., Jia, Y., Chen, Z., Li, J., Wang, G., 2018. Disentangling temperature effects on leaf wax n-alkane traits and carbon isotopic composition from phylogeny and precipitation. Organic Geochemistry 126, 13–22. doi: 10.1016/j.orggeochem.2018.10.008.

Watson, J., Alvin, K.L., 1996. An English Wealden floral list, with comments on possible environmental indicators. Cretaceous Research 17, 5–26. doi: 10.1006/cres.1996.0002.

Waycott, M., McKenzie, L.J., Mellors, J.E., Ellison, J.C., Sheaves, M.T., Collier, C., Schwarz, A.M., Webb, A., Johnson, J.E., Payri, C.E., 2011. Vulnerability of tropical Pacific fisheries and aquaculture to climate change. Pacific Community. chapter Chapter 6: Vulnerability of mangroves, seagrasses and intertidal flatsin the tropical Pacific to climate change.

Welte, D.H., Ebhardt, G., 1968. Distribution of long chain *n*-paraffins and *n*-fatty acids in sediments from the Persian Gulf. Geochimica et Cosmochimica Acta 32, 465–466. doi: 10.1016/0016-7037(68)90080-x.

Wiesenberg, G.L., Lehndorff, E., Schwark, L., 2009. Thermal degradation of rye and maize straw: Lipid pattern changes as a function of temperature. Organic Geochemistry 40, 167–174. doi: 10.1016/j.orggeochem.2008.11.004.

Winter, K., Aranda, J., Holtum, J.A.M., 2005. Carbon isotope composition and water-use efficiency in plants with Crassulacean Acid Metabolism. Functional Plant Biology 32, 381–388. doi: 10.1071/fp04123.

Winter, K., Holtum, J.A.M., 2014. Facultative crassulacean acid metabolism (CAM) plants: powerful tools for unravelling the functional elements of CAM photosynthesis. Journal of Experimental Botany 65, 3425–3441. doi: 10.1093/jxb/eru063.

Yan, C., Zhang, Y., Zhang, Y., Zhang, Z., Huang, X., 2020. Habitat influence on the molecular, carbon and hydrogen isotope compositions of leaf wax n-alkanes in a subalpine basin, central china. Journal of Earth Science 31, 845–852. doi: 10.1007/s12583-020-1322-x.

Zhou, Y., Grice, K., Stuart-Williams, H., Farquhar, G.D., Hocart, C.H., Lu, H., Liu, W., 2010. Biosynthetic origin of the saw-toothed profile in δ^{13}C and δ^{2}Î— of *n*-alkanes and systematic isotopic differences between *n*-, iso- and anteiso-alkanes in leaf waxes of land plants. Phytochemistry 71, 388–403. doi: 10.1016/j.phytochem.2009.11.009.

Zhou, Y., Stuart-Williams, H., Grice, K., Kayler, Z.E., Zavadlav, S., Vogts, A., Rommerskirchen, F., Farquhar, G.D., Gessler, A., 2015. Allocate carbon for a reason: Priorities are reflected in the ^{13}C/^{12}C ratios of plant lipids synthesized via three independent biosynthetic pathways. Phytochemistry 111, 14–20. doi: 10.1016/j.phytochem.2014.12.005.

Čepičková, J., Kvaček, J., 2023, in review. *Papillaephyllum*, a new genus of angiosperm foliage from the Cenomanian of the Czech Republic. Review of Palaeobotany and Palynology 319, 104990. doi: 10.1016/j.revpalbo.2023.104990.

Appendix A. Supplementary material

Table A.4: List of all sampled fossil species with the unit in which they were embedded. The paleoenvironment type is based on sediment characterization by Uličný et al. (1997a).

Fossil species	Sedimentological unit	Palaeoenvironment
Ceratoxylon	U1	Fluvial
Nilssonia mirovanae	U1	Slope
Pseudoctenis babinensis	U1	Slope
Araliaeophyllum sp.	U2	Slope - fluvial
Dicotylophyllum labutae	U2	Slope
Ettingshausenia laevis	U2	Fluvial
Diospiros cretacea	U3	Salt marsh-like, autochthonous
Eretmophyllum obtusum	U3	Salt marsh-like, autochthonous
Frenelopsis alata	U3	Salt marsh-like, autochthonous
Pseudoasterophyllites cretaceus	U3	Salt marsh-like, autochthonous
Eucalyptolaurus sp.	U1, U2	Fluvial and tide-influenced fluvial
Pandemophyllum sp.	U1, U2, U3	Fluvial and tide-influenced fluvial
Dicotylophyllum (Lauroides)	U2, U3	Tide-influenced river
Ascarinophyllum pecinovense	U2, U3	Slope, allochthonous
Sphenolepis pecinovensis	U5	Coastal swamp, autochthonous
Cunninghamites lignitum	U5	Coastal swamp, autochthonous

Figure A.8: Left: A phylogenetic tree showing the phylogeny of all collected plant species. Right: Phylogenetic tree including mean values of environmental variables displayed as centred and scaled values. The size of the square is absolute value of the centred and scaled datapoint, positive value (filled square) means value above average and negative value (empty square) is below average. Crosses show missing data.

Table A.5: Summary of all tested regression models for $\delta^{13}C_{n-C_{29}}$ and salinity

	Intercept	Slope	p-value	R^2	n	df
Linear Model (LM)	-33.8494	0.0273	$3.042 \cdot 10^{-5}$	0.1141	146	144

Generalized Linear	-33.8494	0.0273	$3.04 \cdot 10^{-5}$	0.1141	146	145
Model (GLM)						
Generalized Linear	-34.1323	0.0387	$1.09 \cdot 10^{-3}$	0.076	138	137
Model (GLM) without						
salinity outliers						
Ordinary Least	-33.8494	0.0273	$3.042 \cdot 10^{-5}$	0.1141	281	144
Squares (OLS)						
Phylogenetic Generilized	-34.9197	0.0626	0.253	0.1422	16	9
Least Squares (PGLS)						
Linear Mixing Model	-34.0387	0.0142	0.0034		146,	
with random intercepts					11 species	
(LMM-RI)						
Linear Mixing Model	-34.1218	0.0185	0.043		146,	
with random intercepts					11 species	
and slope effects						
(LMM-RISE)						
Monte Carlo Linear	-33.8494	0.0273	$3.04 \cdot 10^{-5}$		146	145
Model (MCLM)						

Figure A.9: Species and environment specific fractionation factors based on the $\delta^{13}C_{air}$ in the Late Cenomanian (Barral et al., 2017) and present day (He et al., 2021).

Figure A.10: Correlation matrix of all variables for *Avicennia maritima*. Stars show significance of the correlation and numbers are correlation coefficient. Isotopes are represented by $\delta^{13}C_{n-C_{29}}$.

Figure A.11: Correlation matrix of all variables for *Salicornia australis*. Stars show significance of the correlation and numbers are correlation coefficient. Isotopes are represented by $\delta^{13}C_{n-C_{29}}$.

Figure A.12: Correlation matrix of all variables for *Samolus repens*. Stars show significance of the correlation and numbers are correlation coefficient. Isotopes are represented by $\delta^{13}C_{n-C_{29}}$.

Figure A.13: Correlation matrix of all variables for *Glossostigma elatinoides*. Stars show

significance of the correlation and numbers are correlation coefficient. Isotopes are represented by $\delta^{13}C_{n-C_{29}}$.

Figure A.14: Correlation matrix of all variables for *Plantago coronopus*. Stars show significance of the correlation and numbers are correlation coefficient. Isotopes are represented by $\delta^{13}C_{n-C_{29}}$.

Figure A.15: Correlation matrix of all variables for *Plantago lanceolata*. Stars show significance of the correlation and numbers are correlation coefficient. Isotopes are represented by $\delta^{13}C_{n-C_{29}}$.

Figure A.16: Pearson's correlation matrix of all variables in our modern dataset with correlation coefficient. Isotopes are represented by $\delta^{13}C_{n-C_{29}}$.

Figure A.17: Spearman's correlation matrix of all variables in our modern dataset. Stars show significance of the correlation and numbers are correlation coefficient. Isotopes are represented by $\delta^{13}C_{n-C_{29}}$.

Table A.6: Summary of the modern dataset variance significance.

Type of test		isotopes	salinity
t-test paired	species	$p < 2.2 \cdot 10^{-16}$	$p < 2.2 \cdot 10^{-16}$
	locality type	$p < 2.2 \cdot 10^{-16}$	$p < 2.2 \cdot 10^{-16}$
	salinity	$p < 2.2 \cdot 10^{-16}$	–
t-test unpaired	species	$p < 2.2 \cdot 10^{-16}$	$p < 2.2 \cdot 10^{-16}$
	locality type	$p < 2.2 \cdot 10^{-16}$	$p < 2.2 \cdot 10^{-16}$
	salinity	$p < 2.2 \cdot 10^{-16}$	–
F-test	species	$p = 0.35$	$p < 2.2 \cdot 10^{-16}$
		$F = 1.17$	$F = 179.17$
	locality type	$p = 1.18 \cdot 10^{-13}$	$p < 2.2 \cdot 10^{-16}$

		$F = 3.574$	$F = 547.89$
	salinity	$p < 2.2 \cdot 10^{-16}$	–
		$F = 6.523 \cdot 10^{-3}$	–
ANOVA	species	$p < 2.2 \cdot 10^{-16}$	$p = 3.26 \cdot 10^{-4}$
		$F = 25.45$	$F = 3.56$
	salinity	$p = 3.04 \cdot 10^{-5}$	–
		F = 18.55	–
	locality type	$p = 2.62 \cdot 10^{-9}$	$p = 2.48 \cdot 10^{-7}$
		$F = 37.87$	$F = 29.341$

Table A.7: Summary of the variance tests for fossil and recent environments. Two-sample Kolmogorov-Smirnov test in the upper part with D and p values where the null hypothesis is that the two data set have the same distribution. If p-value is below 0.05, the datasets have different distribution and thus are significantly different. The variance test with reported F and p values in the lower part shows the ratio of the variances of two datasets. If F is close to 1, the datasets are not significantly different.

Significance of modern environments and their $\delta^{13}C_{n-C_{29}}$					
	Delta	Salt marsh	Dunes	Transition	Mangrove
Delta	X	D = 0.86	D = 0.57	D = 0.90	D = 0.89
		$p = 5.5 \cdot 10^{-13}$	$p = 0.046$	$p = 2.6 \cdot 10^{-11}$	$p = 4.7 \cdot 10^{-11}$
Salt marsh	F = 0.29	X	D = 0.41	D = 0.26	D = 0.27
	$p = 0.007$		$p = 0.1$	$p = 0.008$	$p = 0.006$
Dunes	F = 0.08	F = 0.29	X	D = 0.43	D = 0.43
	$p = 7.9 \cdot 10^{-5}$	$p = 0.0056$		$p = 0.17$	$p = 0.152$
Transition	F = 0.3	F = 1.03	F = 3.6	X	D = 0.10
	$p = 0.01$	$p = 0.94$	$p = 0.0098$		$p = 0.922$
Mangrove	F = 0.3	F = 1.03	F = 3.6	F = 1.0005	X
	$p = 0.0012$	$p = 0.92$	$p = 0.00099$	$p = 0.99$	
Significance of fossil sedimentary units and their $\delta^{13}C_{n-C_{29}}$					

	U1	U2	U3b	U3c	U5
U1	X	D = 0.12	D = 0.11	D = 0.21	D = 0.24
		$p = 0.43$	$p = 0.215$	$p = 0.03$	$p = 0.04$
U2	F = 0.9	X	D = 0.09	D = 0.25	D = 0.24
	$p = 0.58$		$p = 0.46$	$p = 0.006$	$p = 0.05$
U3b	F = 0.4	F = 0.44	X	D = 0.18	D = 0.16
	$p = 3.8 \cdot 10^{-9}$	$p = 2.6 \cdot 10^{-6}$		$p = 0.02$	$p = 0.3$
U3c	F = 0.33	F = 0.34	F = 1.2	X	D = 0.32
	$p = 3.3 \cdot 10^{-8}$	$p = 3.6 \cdot 10^{-6}$	$p = 0.29$		$p = 0.005$
U5	F = 0.24	F = 0.26	F = 0.6	F = 1.41	X
	$p = 3.3 \cdot 10^{-10}$	$p = 5.1 \cdot 10^{-8}$	$p = 0.013$	$p = 0.19$	
Significance of fossil environments and their $\delta^{13}C_{n-C_{29}}$					
	Swamp	Alluvial plain	Salt marsh-like	Slope	Channel infills
Swamp	X	D = 0.23	D = 0.16	D = 0.33	D = 0.36
		$p = 0.04$	$p = 0.3$	$p = 0.022$	$p = 0.007$
Alluvial plain	F = 2.9	X	D = 0.09	D = 0.22	D = 0.34
	$p = 2.7 \cdot 10^{-7}$		$p = 0.18$	$p = 0.14$	$p = 0.001$
Salt marsh-like	F = 1.7	F = 0.57	X	D = 0.21	D = 0.16
	$p = 0.013$	$p = 2.9 \cdot 10^{-6}$		$p = 0.15$	$p = 0.003$
Slope	F = 6.74	F = 2.3	F = 4.01	X	D = 0.37
	$p = 2.53 \cdot 10^{-7}$	$p = 0.006$	$p = 1.2 \cdot 10^{-5}$		$p = 0.015$
Channel infills	F = 1.72	F = 0.59	F = 1.02	F = 0.25	X
	$p = 0.11$	$p = 0.024$	$p = 0.99$	$p = 0.00019$	

Figure A.18: A heatmap showing the average $\delta^{13}C$ of each *n*-alkane in all the modern samples species. Missing data or not sufficient dataset size are displayed as gray spaces.

Figure A.19: A heatmap showing the average $\delta^{13}C$ of each *n*-alkane in all the fossil samples species. Missing data or not sufficient dataset size are displayed as gray spaces.

Declaration of interests

☐The authors declare that they have no known competing financial interests or personal relationships that could have appeared to influence the work reported in this paper.

☒The authors declare the following financial interests/personal relationships which may be considered as potential competing interests:

Petra Zahajska reports financial support was provided by Charles University Grant Agency. Jiri Kvacek and Jana Cepickova reports financial support was provided by Czech Science Foundation. Petra Zahajska and Jakub Trubac reports financial support was provided by Charles University Center for Geosphere Dynamics.

Highlights:

- The $\delta^{13}C_{n\text{-alkanes}}$ from leaf cuticle provide information on local osmotic stress.
- A positive correlation between water stress and the $\delta^{13}C_{n\text{-alkanes}}$ values of leaf waxes was found.
- The $\delta^{13}C_{n\text{-alkanes}}$ of studied halophytes reflects their flexibility to adapt to osmotic stress.
- The knowledge of modern C3 plant $\delta^{13}C_{n\text{-alkanes}}$ can be applied for interpreting fossil data.
- The $\delta^{13}C_{n\text{-alkanes}}$ from fossil plant cuticles are a useful tool for determining their autecology.

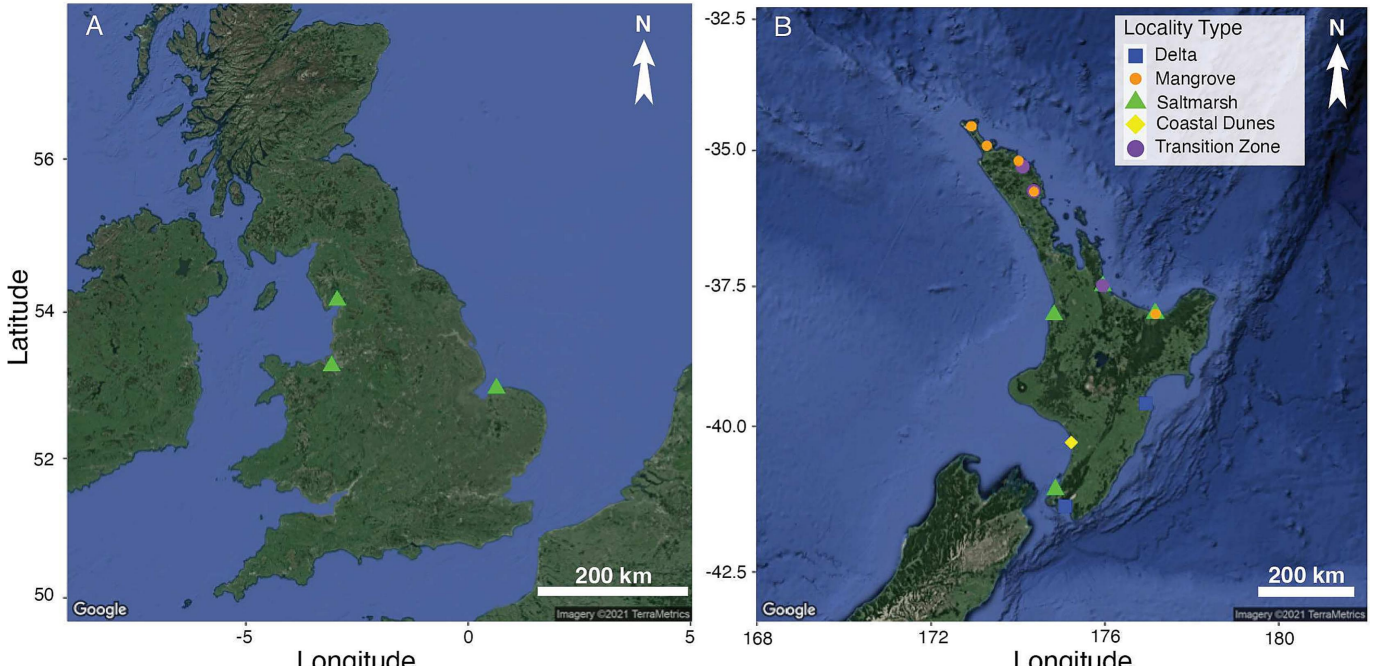
A
N
56
54
52
50
Latitude
-5
0
5
Longitude
200 km
Google
Imagery ©2021 TerraMetrics
B
N
Locality Type
Delta
Mangrove
Saltmarsh
Coastal Dunes
Transition Zone
-32.5
-35.0
-37.5
-40.0
-42.5
168
172
176
180
Longitude
200 km
Google
Imagery ©2021 TerraMetrics

Figure 1

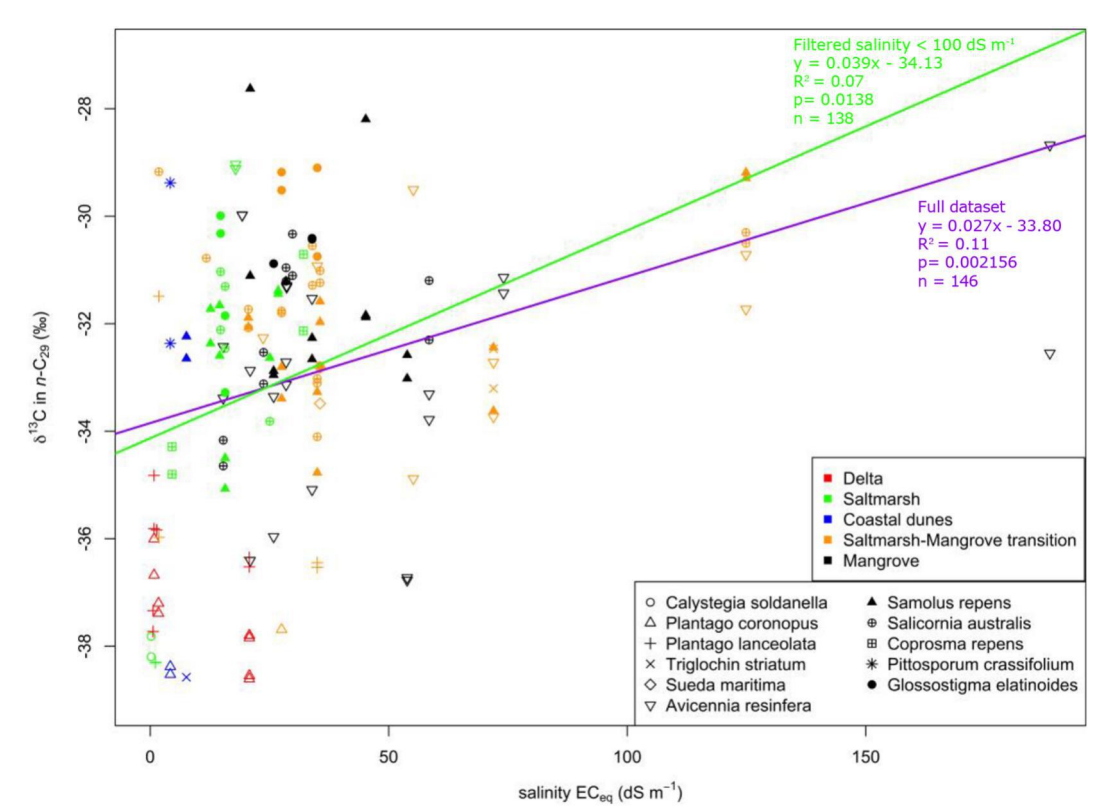
Filtered salinity < 100 dS m-1
y = 0.039x - 34.13
R² = 0.07
p= 0.0138
n = 138
Full dataset
y = 0.027x - 33.80
R² = 0.11
p= 0.002156
n = 146
Delta
Saltmarsh
Coastal dunes
Saltmarsh-Mangrove transition
Mangrove
Calystegia soldanella
Plantago coronopus
Plantago lanceolata
Triglochin striatum
Sueda maritima
Avicennia resinfera
Samolus repens
Salicornia australis
Coprosma repens
Pittosporum crassifolium
Glossostigma elatinoides
δ13C in n-C29 (‰)
salinity ECeq (dS m-1)
-28
-30
-32
-34
-36
-38
0
50
100
150

Figure 2

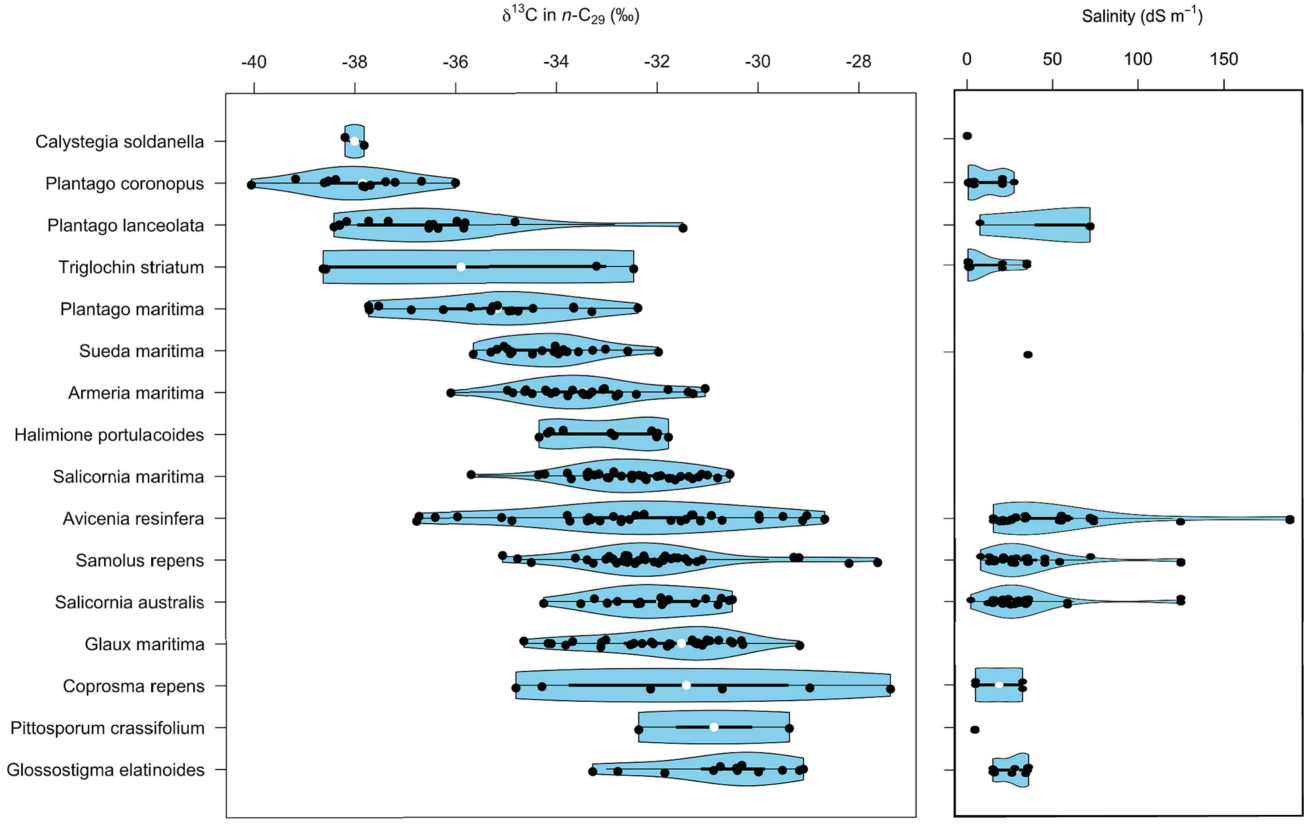
δ13C in n-C29 (‰)
-40
-38
-36
-34
-32
-30
-28
Salinity (dS m−1)
0
50
100
150
Calystegia soldanella
Plantago coronopus
Plantago lanceolata
Triglochin striatum
Plantago maritima
Sueda maritima
Armeria maritima
Halimione portulacoides
Salicornia maritima
Avicenia resinfera
Samolus repens
Salicornia australis
Glaux maritima
Coprosma repens
Pittosporum crassifolium
Glossostigma elatinoides

Figure 3

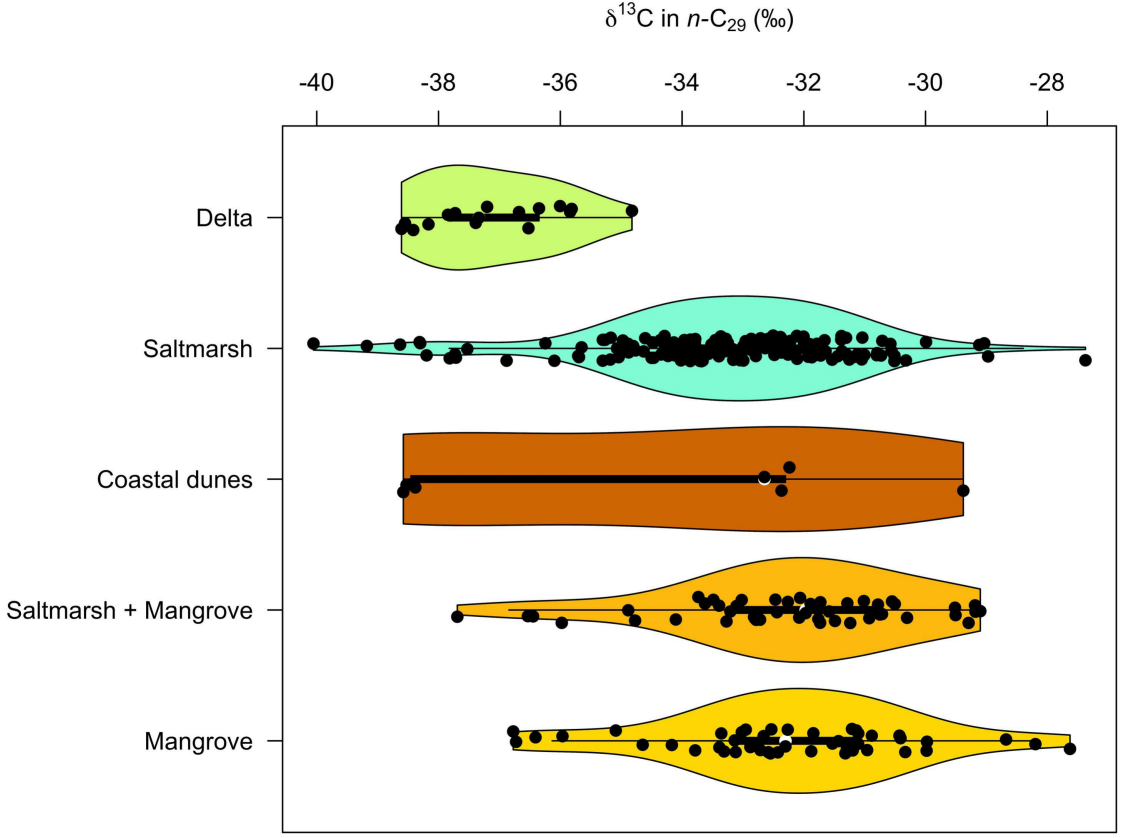
δ13C in n-C29 (‰)
-40
-38
-36
-34
-32
-30
-28
Delta
Saltmarsh
Coastal dunes
Saltmarsh + Mangrove
Mangrove

Figure 4

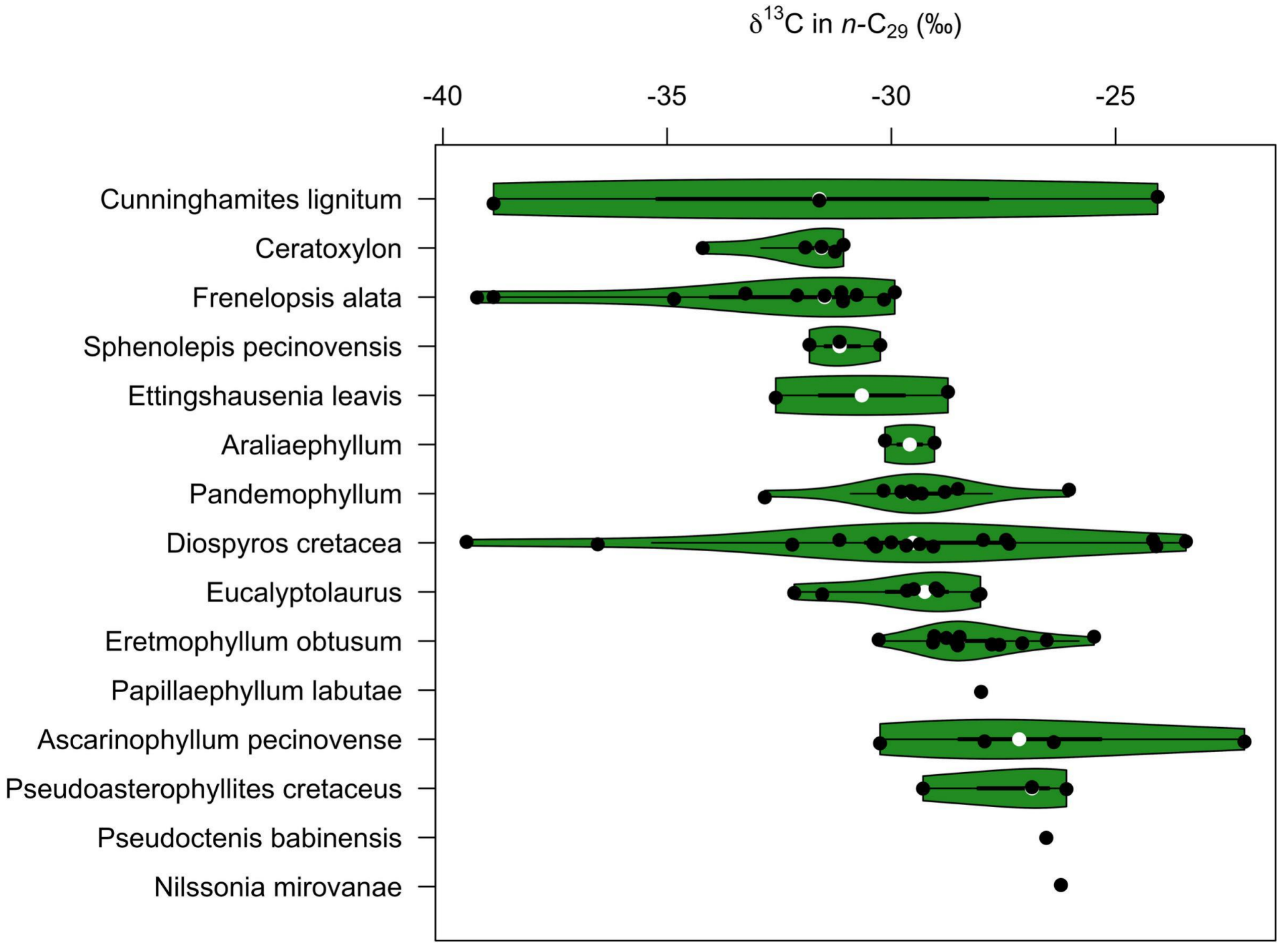
δ13C in n-C29 (‰)
-40
-35
-30
-25
Cunninghamites lignitum
Ceratoxylon
Frenelopsis alata
Sphenolepis pecinovensis
Ettingshausenia leavis
Araliaephyllum
Pandemophyllum
Diospyros cretacea
Eucalyptolaurus
Eretmophyllum obtusum
Papillaephyllum labutae
Ascarinophyllum pecinovense
Pseudoasterophyllites cretaceus
Pseudoctenis babinensis
Nilssonia mirovanae

Figure 5

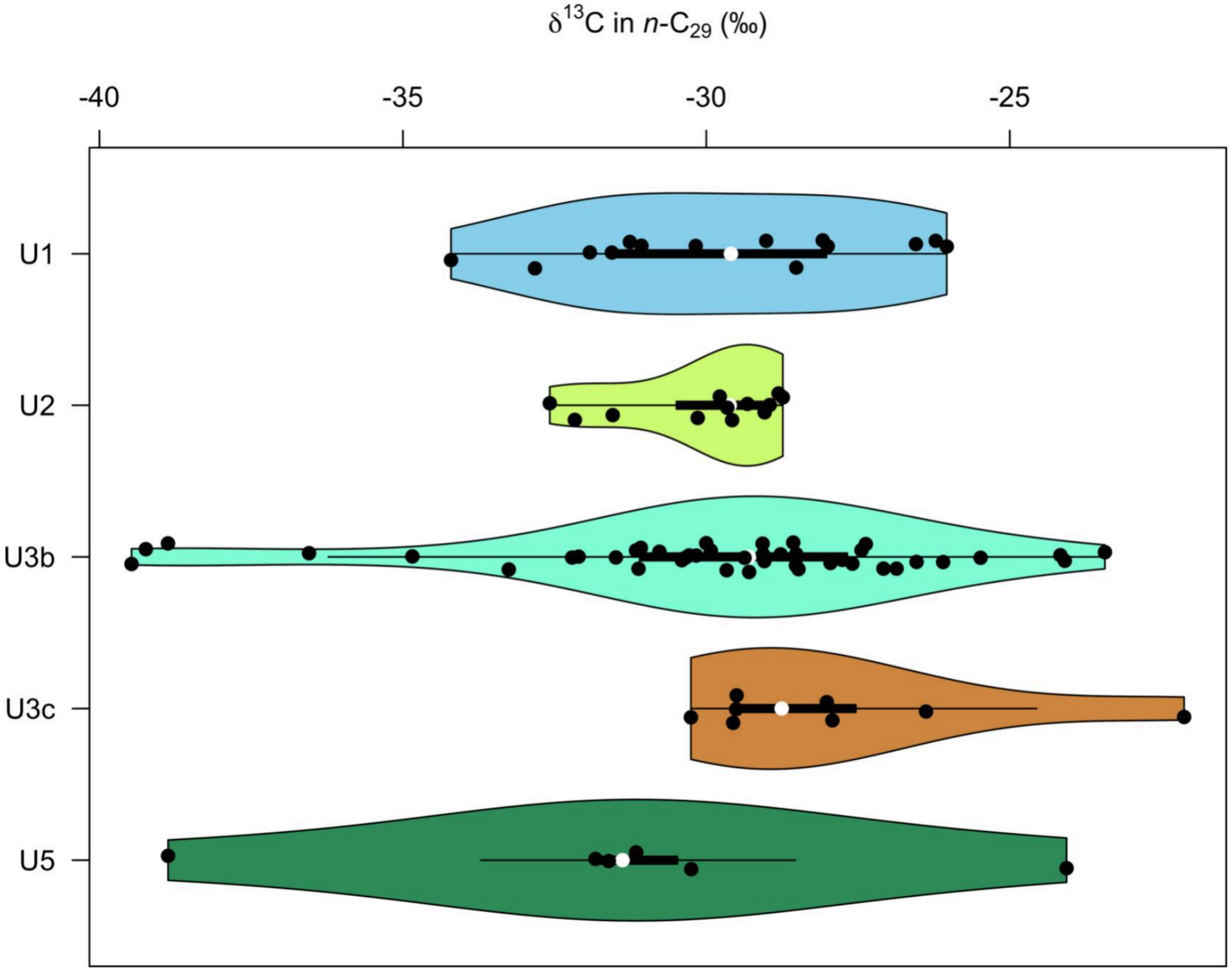

Figure 6


Adapted/presence of some coping strategy to osmotic stress
Low osmotic stress - adaptation
High osmotic stress
Permanent adaptations - halophytes, xerophytes under "standard" stress
Permanent adaptations - halophytes, xerophytes under "extreme" stress
Potentially metabolic pathways switching species (C3 -> CAM)
Some temporary stress tolerance or Adaptive coping mechanisms
Relatively lighter more negative δ13C
Relatively heavier more positive δ13C
Not osmotically stress plants
No adaptation -> incapable to grow in stressed environment
Osmotically stress plants with no adaptation, but
Capable to survive temporarily under stress conditions
Low osmotic stress
High osmotic stress
No adaptation/tolerance to osmotic stress

Figure 7